The Meteoritical Society

Meteoritics & Planetary Science 42, Nr 4/5, 611–633 (2007)
Abstract available online at http://meteoritics.org

Drill core LB-08A, Bosumtwi impact structure, Ghana: Petrographic and shock metamorphic studies of material from the central uplift

Ludovic FERRIÈRE[1*], Christian KOEBERL[1], and Wolf Uwe REIMOLD[2]

[1]Department of Geological Sciences, University of Vienna, Althanstrasse 14, A-1090 Vienna, Austria
[2]Mineralogy, Museum of Natural History, Humboldt University, Invalidenstrasse 43, D-10115 Berlin, Germany
[*]Corresponding author. E-mail: ludovic.ferriere@univie.ac.at

(Received 28 August 2006; revision accepted 29 December 2006)

Abstract–During a recent drilling project sponsored by the International Continental Scientific Drilling Progam (ICDP), two boreholes (LB-07A and LB-08A) were drilled into the crater fill of the Bosumtwi impact structure and the underlying basement, into the deep crater moat and the outer flank of the central uplift, respectively. The Bosumtwi impact structure in Ghana (West Africa), which is 10.5 km in diameter and 1.07 Myr old, is largely filled by Lake Bosumtwi.

Here we present the lithostratigraphy of drill core LB-08A (recovered between 235.6 and 451.33 m depth below lake level) as well as the first mineralogical and petrographic observations of samples from this core. This drill core consists of approximately 25 m of polymict, clast-supported lithic breccia intercalated with suevite, which overlies fractured/brecciated metasediment that displays a large variation in lithology and grain size. The lithologies present in the central uplift are metasediments composed dominantly of fine-grained to gritty meta-graywacke, phyllite, and slate, as well as suevite and polymict lithic impact breccia. The suevites, principally present between 235.6 and 240.5 m and between 257.6 and 262.2 m, display a fine-grained fragmental matrix (about 39 to 45 vol%) and a variety of lithic and mineral clasts that include meta-graywacke, phyllite, slate, quartzite, carbon-rich organic shale, and calcite, as well as melt particles, fractured quartz, unshocked quartz, unshocked feldspar, quartz with planar deformation features (PDFs), diaplectic quartz glass, mica, epidote, sphene, and opaque minerals). The crater-fill suevite contains calcite clasts but no granite clasts, in contrast to suevite from outside the northern crater rim.

The presence of melt particles in suevite samples from the uppermost 25 meters of the core and in suevite dikelets in the basement is an indicator of shock pressures exceeding 45 GPa. Quartz grains present in suevite and polymict lithic impact breccia abundantly display 1 to (rarely) 4 sets of PDFs per grain. The shock pressures recorded by the PDFs in quartz grains in the polymict impact breccia range from 10 to ~30 GPa. We also observed a decrease of the abundance of shocked quartz grains in the brecciated basement with increasing depth. Meta-graywacke samples from the basement are heterogeneously shocked, with shock pressures locally ranging up to 25–30 GPa. Suevites from this borehole show a lower proportion of melt particles and diaplectic quartz glass than suevites from outside the northern crater rim (fallback impact breccia), as well as a lack of ballen quartz, which is present in the external breccias. Similar variations of melt-particle abundance and shock-metamorphic grade between impact-breccia deposits within the crater and fallout impact breccia outside the crater have been observed at the Ries impact structure, Germany.

INTRODUCTION

The 1.07 Myr old Bosumtwi impact structure, centered at 06°30′N, 01°25′W, is located in Ghana, West Africa (Fig. 1). It is a well-preserved, complex impact structure 10.5 km in diameter with a pronounced rim and a small central uplift (Scholz et al. 2002; Koeberl and Reimold 2005). The Bosumtwi impact structure is also associated with the Ivory Coast tektites, on the basis of the geographical location of the tektite strewn field, as well as identical ages and matching chemical and isotopic composition of the tektites and the Bosumtwi crater rocks (Koeberl et al. 1997 and references therein). The crater was excavated in lower greenschist facies metasediments of the 2.1–2.2 Gyr Birimian Supergroup

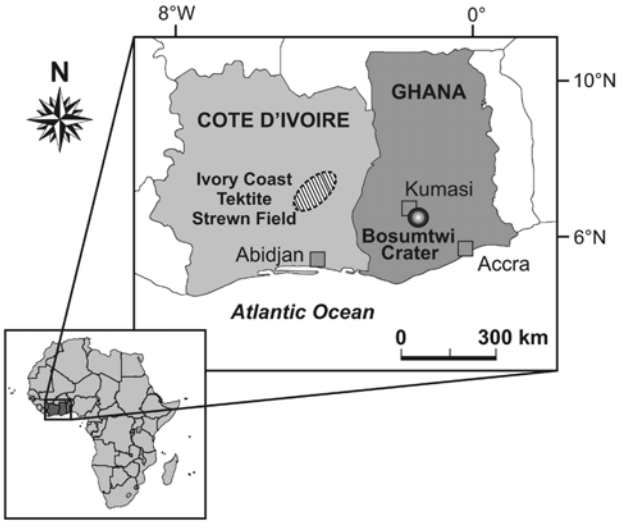

Fig. 1. The geographical location of the Bosumtwi impact crater, Ghana, in relation to the Ivory Coast tektite strewn field (after Koeberl et al. 1998).

(Wright et al. 1985; Leube et al. 1990) and is almost entirely filled by Lake Bosumtwi, which is 8 km in diameter. The lake sediments have accumulated a 1 Myr long paleoclimate record since the impact event. Bosumtwi was recently the subject of an international and multidisciplinary drilling project by the International Continental Scientific Drilling Program (ICDP) (for more information, see below; Koeberl and Reimold 2005; Coney et al. 2006; Ferrière et al. 2006; Koeberl et al. 2006; Koeberl et al. 2007; Coney et al. 2007).

In the present paper, we report on the lithostratigraphy and mineralogy of drill core LB-08A and provide a brief comparison with observations on samples from outside the crater as well as observations at the Ries crater, Germany. Preliminary results were reported in an abstract by Ferrière et al. (2006).

GEOLOGICAL SETTING

First geological investigations around Lake Bosumtwi were made in the 1930s (Junner 1937) and completed later in the 1960s (Woodfield 1966; Moon and Mason 1967; Jones et al. 1981). Recently, additional mapping was carried out to complete and update older observations, which includes descriptions of new outcrops revealed by recent road construction (Koeberl and Reimold 2005). This new geological map also summarizes observations obtained from shallow drilling on and outside of the northern crater rim (Boamah and Koeberl 2003). This work provided a good geological perspective of the crater rim and the region around the crater, but because samples from the crater fill were not accessible due to the lake and lake sediments, that part of the crater remained unknown. The first information on the sublake structure was obtained from aerogeophysical studies (Pesonen et al. 1998, 2003) and seismic investigations (Scholz et al. 2002); the latter revealed the presence of a small central uplift, which was previously only hypothesized.

The crater was excavated in lower greenschist facies metasediments of the 2.1–2.2 Gyr Birimian Supergroup (Wright et al. 1985; Leube et al. 1990). The rocks from this supergroup were previously separated into Lower and Upper Birimian units, dominated by metasediments and metavolcanics, respectively (Junner 1937), but this subdivision has recently been abandoned (Koeberl and Reimold 2005). These rocks are an assemblage of metasediments that comprises phyllites, meta-tuffs, meta-graywackes, quartzitic meta-graywackes, schists (see Coney et al. 2007), shales, and slates. Birimian metavolcanic rocks occur to the southeast of the crater and Tarkwaian clastic sedimentary rocks (detritus of Birimian rocks) occur to the east and southeast of the crater (Koeberl and Reimold 2005). A variety of intrusive bodies has also been observed around the crater, including Proterozoic granitic intrusions, weathered granitic dikes, other granitoid dikes, and dolerite and amphibolite dikes (e.g., Junner 1937; Woodfield 1966; Moon and Mason 1967; Reimold et al. 1998). Some of these intrusions seem to be correlated with the Pepiakese and Kumasi intrusive bodies (Woodfield 1966; Moon and Mason 1967). Several outcrops of breccia were described from around the crater (e.g., Junner 1937; Woodfield 1966; Moon and Mason 1967), but it is not clear whether or not all these breccias are impact-related (Reimold et al. 1998). On the basis of composition and texture, Boamah and Koeberl (2003) distinguished three types of impact breccia at the Bosumtwi crater: an autochthonous monomict breccia, a probable allochthonous polymict lithic impact breccia, and a suevitic breccia. Monomict breccia occurs along the northern crater rim and consists of angular fragments of different sizes, irregularly distributed and cemented in a matrix of the same materials (Boamah and Koeberl 2003). Previously suevite has been found outside of the northern and southern crater rim (at about 250 m to 2 km from the crater rim crest) (Koeberl and Reimold 2005); this suevite contains abundant impact-melt fragments and a variety of clasts (meta-graywacke, phyllite, shale, granite) up to about 40 cm in size (Boamah and Koeberl 2003, 2006).

THE 2004 ICDP DRILLING PROJECT

The ICDP drilling project had two major scientific goals: to obtain a 1-million-year paleoenvironmental record from post-impact sediments and to acquire hardrock samples from the central uplift and crater moat of the largest young impact structure known on Earth. During this project, sixteen drill cores were obtained at six locations in the lake. Drilling, geophysical studies, and logging were done between June and October 2004 (see Koeberl et al. 2007). Fourteen sediment cores were drilled for paleoenvironmental studies and two

impactite cores (LB-07A and LB-08A) were drilled for impact crater investigations. Note that all sample depths used in this paper represent depths below lake level. These two boreholes (LB-07A and LB-08A) were drilled into the crater fill and underlying basement to depths of 545.08 m in the deep crater moat and to 451.33 m depth on the outer flank of the central uplift, respectively. Their locations, 6°30′50″N, 1°24′55″E for LB-07A and 6°30′33″N, 1°24′45″E for LB-08A, are situated on lines of seismic surveys that were made during the preparation phase of the drilling project (Karp et al. 2002; Scholz et al. 2002).

In this study we focus on core LB-08A, which was recovered at a depth between 235.6 and 451.33 m and represents 215.7 m of core with a diameter of 6 cm. The core sections are stored at the ICDP headquarters (GeoForschungsZentrum [GFZ] in Potsdam, Germany) in 73 boxes. Depending on the rock types and alteration level of the rocks, core recovery ranged from 40 to 115%, with an average of 93%. Cores were scanned and documented in December 2004 and January 2005 at the GFZ. Core images, scanning data, and detailed core descriptions are available online at http://bosumtwi.icdp-online.org.

SAMPLES AND EXPERIMENTAL METHODS

One hundred and twenty one samples were taken from core LB-08A, covering depths from 235.77 m (KR8-001) to 451.23 m (KR8-125) (see Appendix 1 for depths of all the samples). Samples were selected to encompass the complete variety of different lithologies present. The petrographic characteristics of the samples, including shock metamorphic effects, were studied by optical and electron microscopy. For this purpose, 174 unoriented thin sections (representing 53 impact breccia and 121 metasediment samples) were prepared from the 121 samples and investigated by optical microscopy. In addition, 12 polished thin sections were prepared for electron microscopy. Electron microscopy, including mineral analysis by energy-dispersive spectrometry (EDX), was done with a JEOL JSM 6400 instrument at the Naturhistorisches Museum, Vienna, Austria, at 15 kV acceleration voltage and with a beam current of about 2 nA. The EDX analyses have a precision of about 3 rel% and a detection limit of about 0.1 wt% for major elements. In addition, electron microprobe analyses were obtained at the Commissariat à l'Energie Atomique (CEA), Gif-sur-Yvette, France, using a JEOL JSM 840 scanning electron microscope (SEM) associated with an energy-dispersive spectrometer (EDS). Chemical analyses were done at 15 kV acceleration voltage with 1 nA sample current and a beam diameter of 1 µm. Multi-element spectra obtained from the SEM/EDS-ACC system were compared to a series of pure reference spectra, and X-ray absorption and fluorescence effects were corrected using the ZAF program supplied by Princeton Gamma Tech (PGT). The precision is about 5 rel% and the detection limit is 0.1 wt%.

For each sample, lithology, minerals present, and shock effects in these minerals were assessed qualitatively. In addition, modal analyses of 9 suevite thin sections (from samples between 235.77 and 260.49 m) were made by point-counting. The petrographic "point-counting" method used in this study is not the one traditionally used (e.g., Chayes 1949), but an alternative method based on estimation of the true values of areal fractions. This new method was employed because of the counting error due to the large particle size (lithic and mineral clasts). In this method, the area of the whole thin section was subdivided into adjacent cells of 2.4 × 1.5 mm (equivalent to a rectangle in the field of view of the microscope at a magnification of 50×). Each one of those "cells" was further subdivided into three smaller rectangles of identical size (1.5 × 0.8 mm, i.e., an area of 1.2 mm^2). The type of clast/aggregate(s) in each of these rectangles was determined and their number was counted. Only clasts and aggregates with long dimensions ≥0.8 mm were counted as such, and anything smaller than this limit was considered to be "matrix." This method is intermediate between the traditional petrographic modal analysis (e.g., Chayes 1949) and digital image analysis of thin section microphotographs. The reason for choosing this technique was the large size of the clasts in the suevites; thus it is only applicable to rocks with populations of large clasts. Between 566 and 676 areas of 1.2 mm^2 were counted per thin section.

Measurements of the crystallographic orientations of planar deformation features (PDFs) in quartz grains (e.g., Stöffler and Langenhorst 1994; Grieve et al. 1996) with a four-axis universal stage (U-stage; cf. Reinhard 1931; Emmons 1943) were made in individual quartz grains of 10 thin sections. The optic axis and the pole to a PDF plane were determined, and PDFs were indexed in a stereonet with the c-axis in the center (Engelhardt and Bertsch 1969; Stöffler and Langenhorst 1994; Langenhorst 2002). The PDF poles were indexed with Miller indices (hkil) for quartz using the technique described in Stöffler and Langenhorst (1994). Five Raman spectra were determined in two samples with a Renishaw Invia Raman spectrometer at the Laboratoire de Géologie (ENS-Paris, France) to confirm the occurrence of carbon and the carbon organization-state in a specific clast population present in suevite samples. An excitation wavelength of 514 nm was used on a 20 mW Ar laser. The laser beam was focused by a microscope equipped with a LEICA 50× magnification objective, leading to a spot diameter of 1 micrometer. Acquisition time was 10 s for all measurements.

RESULTS

Core LB-08A—Introduction and Terminology

Based on our macroscopic and microscopic observations (Appendix 1), we constructed a detailed lithostratigraphic column of drill core LB-08A (Fig. 2). This drill core displays

a variety of lithologies: polymict breccia, monomict lithic breccia, slate, phyllite, and meta-graywacke. It can also be divided into two main parts: the uppermost 25 meters that are composed of polymict lithic impact breccia (clast-supported) intercalated with suevite, and the other part of the core (between 262 to 451 m), which is dominated by fractured/brecciated metasediment, locally intersected by monomict lithic breccia and suevite dikelets (Fig. 2). Metasediment displays a large variation in lithology (slate, phyllite, and meta-graywacke) and grain size (from fine-grained to gritty meta-graywacke). In order of abundance, the LB-08A drill core intersected about 65% meta-graywacke, 21% slate and phyllite, 13.5% polymict breccia, and 0.5% monomict lithic breccia (estimations based on our macroscopic core descriptions).

Our classification of the various rock types follows definitions by Stöffler and Grieve (1994) for impact breccia, and Jackson (1997) and Brodie et al. (2004) for metasediments. Suevite is defined as a "polymict impact breccia with clastic matrix containing lithic and mineral clasts in various stages of shock metamorphism including cogenetic impact melt particles which are in a glassy or crystallized state" (Stöffler and Grieve 1994). Polymict lithic impact breccia contains shocked and unshocked clasts from more than one precursor lithology in a clastic matrix, but lacks cogenetic melt particles. Monomict lithic impact breccia is defined as a "cataclasite produced by impact and generally displaying weak or no shock metamorphism; occurs in the (par)autochthonous basement of an impact crater or as clasts (up to the size of blocks and megablocks) within allochthonous impact breccias" (Stöffler and Grieve 1994). Schist is "the systematic root term covering all rocks with a well-developed schistosity including slates and phyllites" (Brodie et al. 2004). Slate is "a compact, fine-grained metamorphic rock that possesses slaty cleavage and hence can be split into slabs and thin plates. Most slate was formed from shale" (Jackson 1997). Phyllite is "a metamorphosed rock, intermediate in grade between slate and mica schist. Minute crystals of graphite, sericite, chlorite impart a silky sheen to the surface of cleavage (or schistosity). Phyllites commonly exhibit corrugated cleavage surfaces" (Jackson 1997). Graywacke is "a dark gray firmly indurated coarse-grained sandstone that consists of poorly sorted angular to subangular grains of quartz and feldspar, with a variety of dark rock and mineral fragments embedded in a compact clayey matrix and containing an abundance of very fine-grained illite, sericite, and chloritic minerals" (Jackson 1997). In this paper, we use the term "meta-graywacke," because all graywacke is metamorphosed.

Detailed Lithostratigraphy of Core LB-08A

Polymict Lithic Impact Breccia

Polymict lithic impact breccia intercalated with suevite (Fig. 3a) is present between 235.6 to 262 m. The polymict lithic impact breccia is clast-supported and consists of angular to subrounded rock fragments of a variety of sizes (from <1 to >6 cm, the diameter of the core). These fragments represent three different lithologies, in order of decreasing abundance: meta-graywacke, phyllite, and slate. Thin section observations (see Appendix 1 for detailed descriptions of all samples) confirm the presence of these fragment types, but also the occurrence of quartzitic fragments (up to 6 vol% in KR8-008; depth = 244.45 m). The matrix is fine-grained and grayish in color, consisting of small lithic fragments and metasedimentary minerals, as well as secondary minerals such as phyllosilicates. The abundance of matrix varies from less than 1 vol% (e.g., in KR8-009; depth = 244.87 m) to 5 vol% (e.g., in KR8-015 and KR8-017; depth = 250.74 m and 251.74 m, respectively), and up to 48 vol% (in KR8-008; depth = 244.45 m). Polymict lithic breccia samples are altered (e.g., KR8-009; depth = 244.87 m); most of the biotite (present principally in meta-graywacke clasts) is altered to chlorite and some feldspar to sericite (with presence of cloudiness). This alteration is variable in the samples (from 50 to 80 vol% of feldspar altered to sericite) and no trend of increasing or decreasing alteration degree with depth was observed. The alteration is localized preferentially along fractures. Aggregates of very fine-grained calcite, veinlets, and veins are frequently observed in polymict lithic impact breccia (e.g., KR8-022; depth = 256.81 m), and also some cracks/fractures are filled with iron oxides, pyrite, and rutile (e.g., KR8-024; depth = 259.14 m). Calcite veinlets, as well as fractures filled with iron oxides, are irregularly distributed through the polymict lithic impact breccia and represent less than 5 vol% of the core.

Suevite

General Aspects: The polymict lithic impact breccia between 235.6 to 262 m is intercalated with suevite. Suevite is not easily distinguished from polymict lithic breccia at the macroscopic scale (Figs. 3b and 3c) due to the low abundance of melt particles and their small size. On a macroscopic scale in hand specimen, the melt particle abundance in the suevite appears to be <1 vol%, but microscopic studies of thin sections yields higher values of up to about 15 vol%. Suevite samples have a grayish, fine-grained fragmental matrix and consist of rock and mineral clasts and of secondary minerals like smectite, chlorite, and calcite, in the form of very fine-grained aggregates or micro-veinlets. Matrix accounts for 39 to 45 vol% of the total suevite (Fig. 4; Table 1). A variety of lithic and mineral clasts, with sizes up to 5 cm, is present: meta-graywacke, phyllite, slate, quartzite, carbon-rich organic shale, and calcite. Furthermore, there are melt particles, fractured quartz, unshocked quartz, unshocked feldspar, quartz with PDFs, diaplectic quartz glass, micas, epidote, sphene, and opaque minerals. For more details about the clast distribution in the top 25 meters of the core, see Fig. 4 and Table 1.

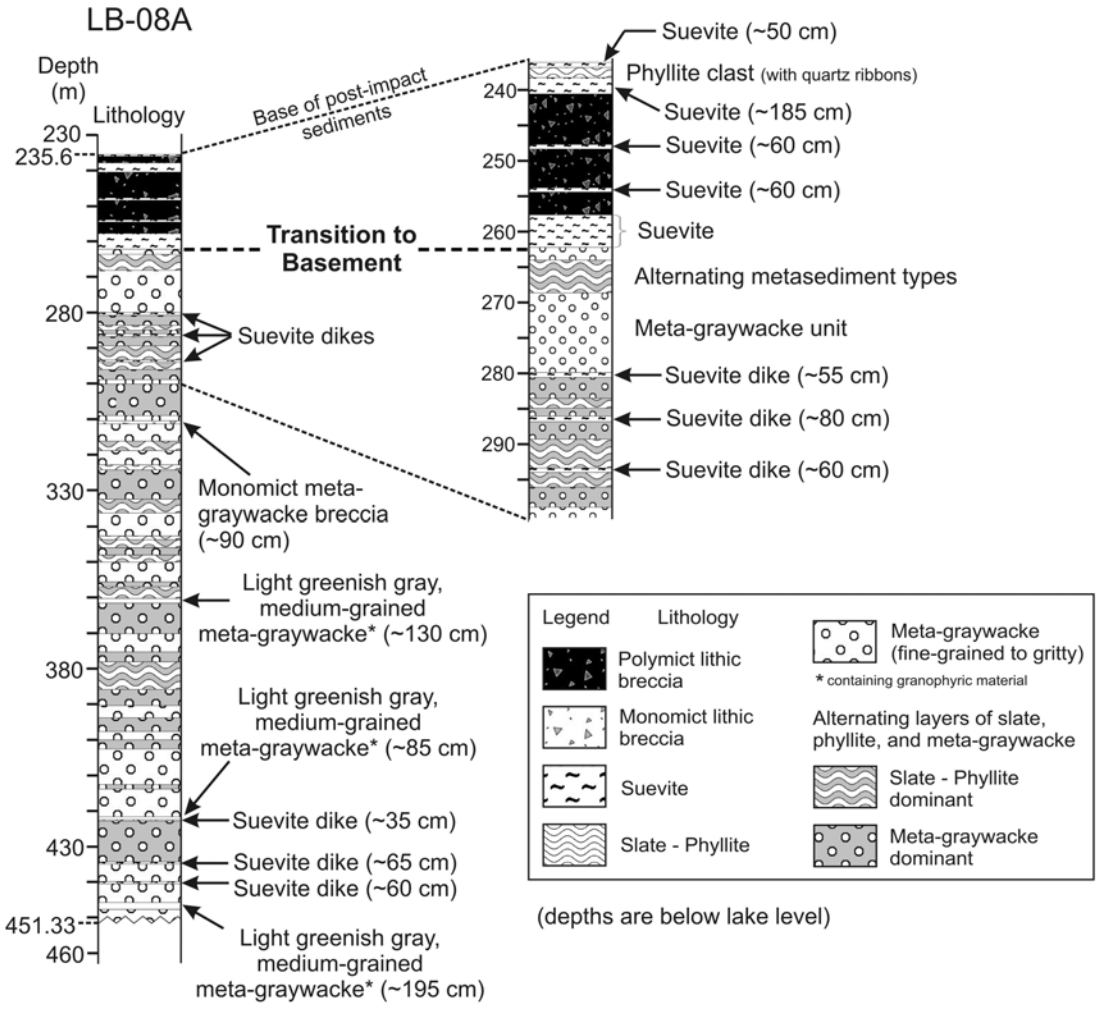

Fig. 2. A detailed lithostratigraphic column of drill core LB-08A. The uppermost 25 m are composed of clast-supported polymict lithic impact breccia intercalated with suevite (interpreted as fallback breccia). The lower part of the core is composed of an alternating sequence of metasediment with (in order of decreasing abundance) meta-graywacke (dominant), phyllite, and slate; locally monomict lithic breccia; light greenish gray, medium-grained meta-graywacke (with granophyric material); and suevite dikelets in the metasediment. Metasediment displays a large variation in lithology and grain size. This second part of the core, between 262 to 451 m, represents the basement that has been shocked and fractured during the impact crater formation. The transition to basement is at a depth of about 262 m below lake level.

Lithic Clasts, Melt Particles, and Diaplectic Quartz Glass:

Meta-graywacke clasts display a variety of grain sizes (from fine- to medium-grained, and rarely to gritty) and also a variety of textures that include meta-graywacke with strong mylonitic fabric, sheared meta-graywacke, and undeformed meta-graywacke. The abundance of the meta-graywacke clasts in the suevite ranges from ~17.5 vol% to more than 42 vol% of the total suevite in samples between 235.77 to 260.49 m depth (Fig. 4; Table 1). Meta-graywacke clasts are more altered in the uppermost 5 meters.

Point-counting confirms that lithic clasts in suevite are dominated by meta-graywacke and that the clasts are seemingly irregularly distributed throughout the suevite section. Phyllite and slate clasts are more or less abundant (from ~5 to 30 vol%), and the phyllite clasts frequently display crenulation.

Carbon-rich shale clasts (Fig. 5) are only present in the uppermost few meters of the core (in samples KR8-001, KR8-003, KR8-004, KR8-005, and KR8-012), with a slightly decreasing abundance with increasing depth (from 7 to 2 vol%) (Fig. 4; Table 1). The presence of carbon in the clast population termed “carbon-rich shale clast” was confirmed by Raman spectra obtained for four carbon-rich shale clasts in two samples (KR8-003 and KR8-005; depths = 238.90 and 240.04 m, respectively). The Raman spectra display a typical carbon signature with one intrinsic band (G-band, 1582 cm^{-1}) originating from the lattice vibration of graphite, in addition to a defect-induced band (D-band, 1355 cm^{-1}) (Fig. 5). The intensity ratios between these two bands (used to evaluate the structural ordering of carbonaceous matter) (see Wopenka and Pasteris [1993] for more information) indicate that the carbon is not well organized.

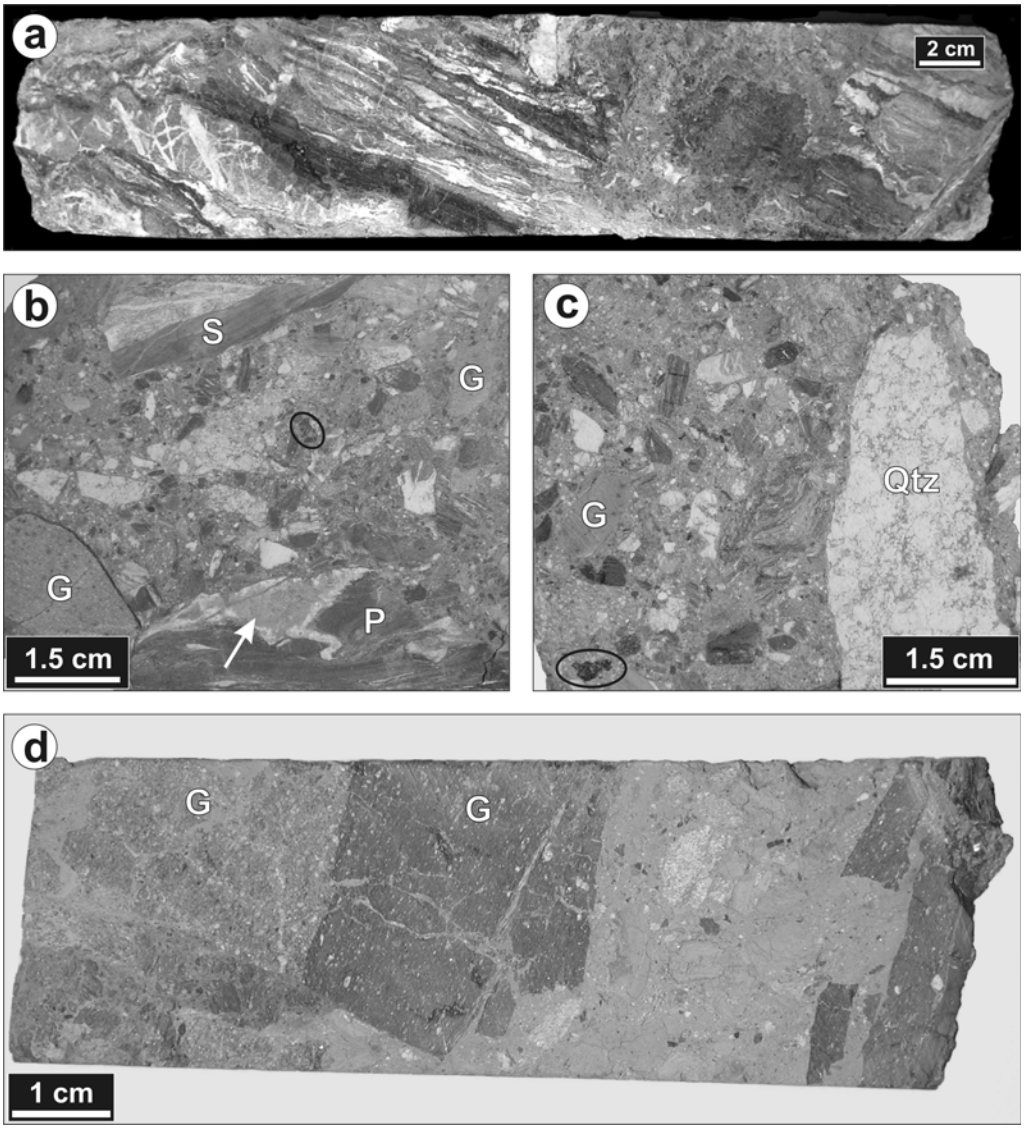

Fig. 3. Macrophotos. a) Polymict lithic impact breccia. Sample KR8-011; depth = 247.46 m. b) Suevite with variety of lithic clasts: meta-graywacke (G), phyllite (P), and slate (S), glass (arrow), melt particles (see ellipse), carbon-rich organic shale, quartzite, and calcite. Sample KR8-001; depth = 235.77 m. c) Suevite (similar to [b]), but with a prominent quartzite (Qtz) clast and a distinct melt particle (see ellipse). Sample KR8-003; depth = 238.90 m. d) Strongly altered suevite with prominent meta-graywacke clasts (fine- to medium-grained) and secondary phyllosilicates. Sample KR8-043; depth = 296.94 m.

Quartz, feldspar, and calcite fragments (mainly with angular shape) are also present in the suevite, with average abundances of 2 vol%, 1 vol%, and <1 vol%, respectively (Fig. 4; Table 2). Feldspar grains frequently display polysynthetic twinning displaced along microfaults that could be tectonic or impact derived. Several calcite grains display anomalously dense cleavage and some planar fractures (Fig. 11a), up to four different directions per calcite grain. These planar fractures in calcite are not yet understood, but could represent impact-induced deformation.

Melt particles, which are usually not observed in hand specimen, are rare in the suevite samples (Fig. 3), comprising ~6 vol% on average in suevite from 235.77 to 260.49 m, with maximum abundances of 10–15 vol% observed in samples KR8-004, KR8-005, and KR8-026 (Fig. 4; Table 1). Mostly devitrified melt particles, in which the original glass is rarely preserved, occur at various stages of alteration, from partially to completely transformed to secondary phyllosilicates (Figs. 6a and 7). Melt particles are subangular, or subrounded to irregular, in shape, and most have sizes between 100 µm and 0.5 cm; the largest melt particle observed is ~1 cm, in sample KR8-004; depth = 239.65 m. Some lithic quartz clasts are common within melt particles (Figs. 6a and 7). These quartz fragments, most of them shocked, display planar fractures (PFs) and PDFs with altered, originally likely amorphous material (Fig. 7).

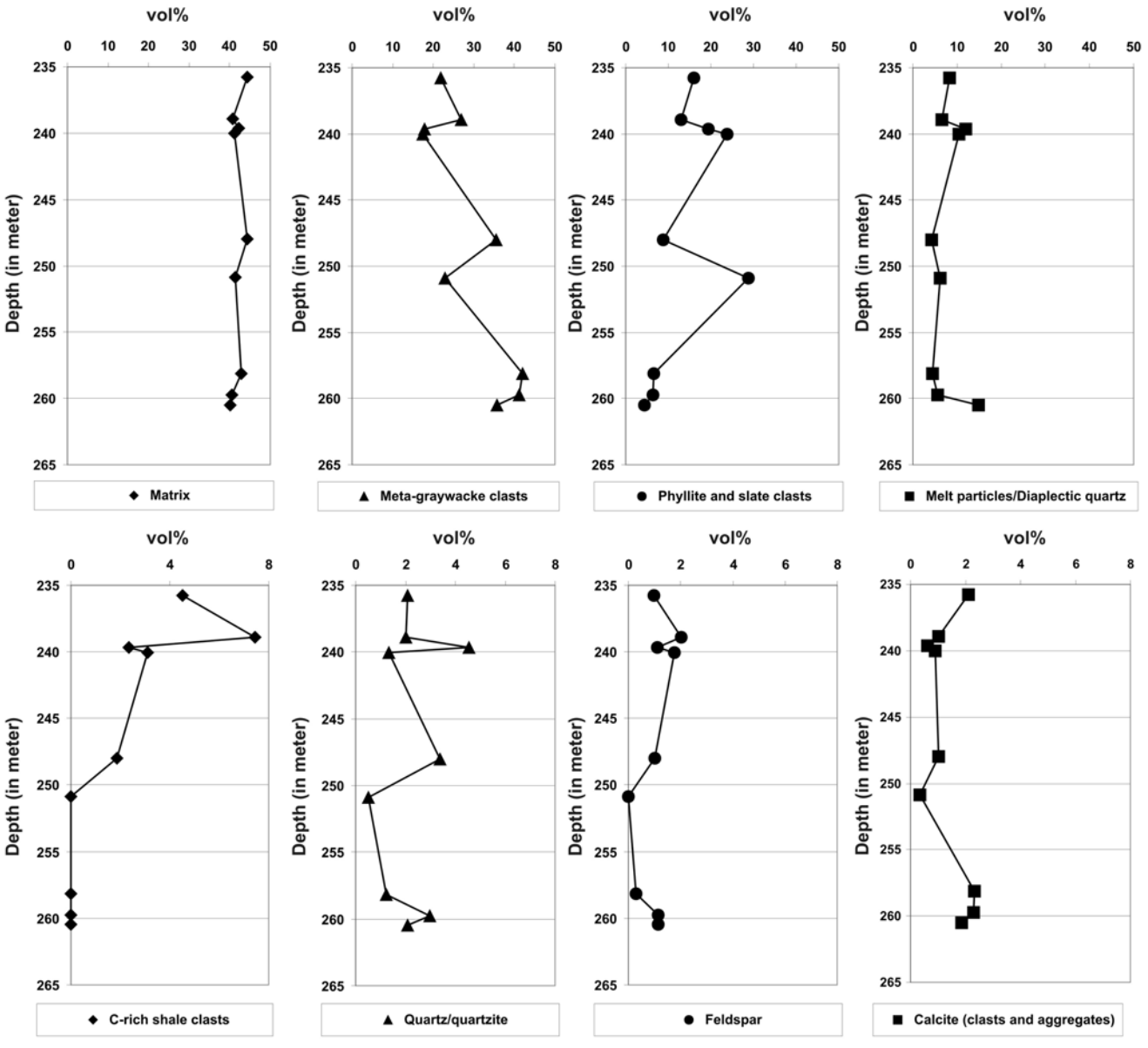

Fig. 4. Modal compositions (vol%) of nine suevite samples from core LB-08A between 235.77 and 260.49 m (between 566 and 676 areas of 1.2 mm^2 were counted per thin section).

Diaplectic quartz glass (Fig. 8) has only been observed in the uppermost 5 m of suevite (in KR8-001 and KR8-005; depths = 235.77 and 240.04 m, respectively). Two diaplectic quartz glass fragments present in KR8-001 (2 and 8 mm in size, respectively) contain altered silicate and residual quartz grains that display PFs where the originally amorphous material is altered only in part.

Shock Petrographic Study: Shock-metamorphic effects in rocks are the main characteristics by which an impact origin is assigned to a circular geological structure (e.g., Stöffler and Langenhorst 1994; Huffman and Reimold 1996; French 1998; Montanari and Koeberl 2000). In the case of Bosumtwi, the first evidence for an impact origin came from findings of NiFe-rich spherules (e.g., El Goresy et al. 1968) and of the high-pressure quartz polymorph coesite (Littler et al. 1961). Later, PDFs in quartz and feldspar were found in suevite outside of the northern crater rim (e.g., Koeberl et al. 1998; Boamah and Koeberl 2003; Koeberl and Reimold 2005).

A variety of shock-petrographic effects has been observed in suevite samples from core LB-08A, including melt particles, diaplectic quartz glass, and PDFs in quartz grains.

Quartz grains with PFs and PDFs (commonly 1, 2, or 3 sets; rarely 4 sets) are present in suevite. Some of these quartz grains have a grayish brown appearance in plane-polarized light (Figs. 9a and 9b), with patches containing micrometer-

Table 1. Modal compositions (vol%) of nine suevite samples from core LB-08A between 235.77 and 260.49 m (counting of 566 to 676 areas of 1.2 mm^2 per thin section). Only clasts/aggregates with long dimensions ≥0.8 mm were counted. Any clast/aggregate or crystal smaller than this size limit was counted as matrix.

Sample	KR8-01	KR8-03	KR8-04	KR8-05	KR8-12	KR8-16	KR8-23	KR8-25	KR8-26
Depth (m)	235.77	238.90	239.65	240.04	248.00	250.89	258.14	259.74	260.49
Matrix	44.3	40.8	42.2	41.3	44.4	41.4	42.8	40.5	40.0
Meta-graywacke clasts	21.8	26.9	17.9	17.5	35.5	22.8	42.0	41.2	35.7
Phyllite and slate clasts	16.0	13.1	19.3	23.8	8.8	28.9	6.6	6.4	4.4
Melt particles and diaplectic quartz	8.2	6.6	11.9	10.4	4.2	6.1	4.5	5.6	14.8
C-rich shale clasts	4.5	7.5	2.4	3.1	1.9	0	0	0	0
Quartz/quartzite	2.1	2.0	4.6	1.3	3.4	0.5	1.2	3.0	2.1
Feldspar	1.0	2.0	1.1	1.8	1.0	0	0.3	1.2	1.2
Calcite (clasts and aggregates)	2.1	1.0	0.6	0.9	1.0	0.3	2.3	2.3	1.9

size fluid inclusions; this has been described as a "toasted appearance" (Short and Gold 1996; Whitehead et al. 2002). Other quartz grains display PDFs decorated with numerous small fluid inclusions (Fig. 9). Traditionally, decorated PDFs are considered secondary features, formed by annealing and aqueous alteration of non-decorated amorphous PDFs (Grieve et al. 1996; Leroux 2005). The crystallographic orientations of 151 sets of PDFs in 82 quartz grains (methods in, e.g., Stöffler and Langenhorst 1994; Grieve et al. 1996) were analyzed on 5 thin sections of suevite (KR8-001, KR8-003, KR8-004, KR8-005, and KR8-006; depth = 235.77, 238.90, 239.65, 240.04, and 240.36 m, respectively; Table 2a). The frequency of indexed PDFs versus angle between c-axis and PDFs, with only indexed planes (Grieve et al. 1996), is shown in Fig. 10a. Between 60 to 68 rel% of all the poles to the PDF planes measured are oriented about 23° to the c-axis, corresponding to the $\omega\{10\bar{1}3\}$ orientation that is diagnostic of shock metamorphism (e.g., Stöffler and Langenhorst 1994; Grieve et al. 1996). Planes parallel to the $\{22\bar{4}1\}$, $\{11\bar{2}2\}$, $\{10\bar{1}1\}$, $\{10\bar{1}2\}$, and $\{11\bar{2}1\}$ orientations are also present (between 2 and 8 rel%) and only about 10 rel% of the measured sets could not be indexed. Only a very small component (<2 rel%) of basal PDFs was found. More detail on the shock effects in quartz, as determined by transmission electron microscopy (TEM) analysis, will be presented elsewhere. No PDFs were observed in feldspar grains.

Basement Rocks

General Aspects: Most of the core recovered from 262 to 451.33 m consists of an alternating sequence of metasediments, in order of decreasing abundance: meta-graywacke (dominant), phyllite, and slate. Suevite dikelets (3 dikelets between 279.5 and 298 m and 3 other dikelets between 418 and 440 m; up to 80 cm thick), monomict meta-graywacke breccia (between 310 and 311 m), and a distinct light greenish gray, medium-grained meta-graywacke (containing granophyric material) are also present in the basement (Fig. 2). Basement rocks display a high number of fractures that are irregularly distributed throughout the basement rocks. Quartz veinlets and veins (from the millimeter-scale to 25 cm thickness; KR8-111, depth = 432.03 m) are also present and irregularly distributed in the lower part of the core. Locally meta-graywacke is completely brecciated (e.g., presence of monomict meta-graywacke breccia, between 310 and 311 m), and in other parts, meta-graywacke samples display disking (possibly related to drilling; e.g., in between 269 and 272 m; Deutsch et al. 2007).

Meta-graywacke: Meta-graywacke is light to dark gray in color and occurs with a large variability of grain size, from fine-grained to gritty (Fig. 12; Appendix 1). The term gritty is used for grain sizes larger than 5 mm. This variability of grain size is noted in hand specimen as well as at the thin-section scale (Fig. 13), which makes it difficult to construct a lithostratigraphic column at a reasonable scale. Meta-greywacke samples show undeformed, sheared, brecciated, and mylonitic textures (Appendix 1) and are mainly composed of (in order of decreasing abundance): quartz, feldspar, muscovite, chlorite/biotite, calcite, and accessory minerals (in order of decreasing abundance: epidote, pyrite, sphene, apatite, zircon, rutile, allanite). In most of the samples, biotite is altered to chlorite. Some meta-graywacke samples have significant carbonate content, in the form of numerous aggregates of very fine-grained calcite, veinlets, and veins (e.g., KR8-053 and KR8-122, depths = 316.97 and 446.69 m, respectively) (Appendix 1), with variable amounts in each sample (see variations with depth of CaO abundances measured in bulk samples) (Ferrière et al. 2007). meta-graywacke samples display also a variability of relative abundances of quartz, feldspar, and mica, which is difficult to quantify by optical observations alone, but the variations in the abundances of silica and aluminum measured in bulk samples (see Ferrière et al. 2007) illustrates such compositional variations throughout the core. Quartz grains frequently show microfractures and undulatory extinction. Feldspar grains also display some cracks and are commonly altered to sericite. Most meta-graywacke samples are shocked (PFs and PDFs in quartz grains; see details below).

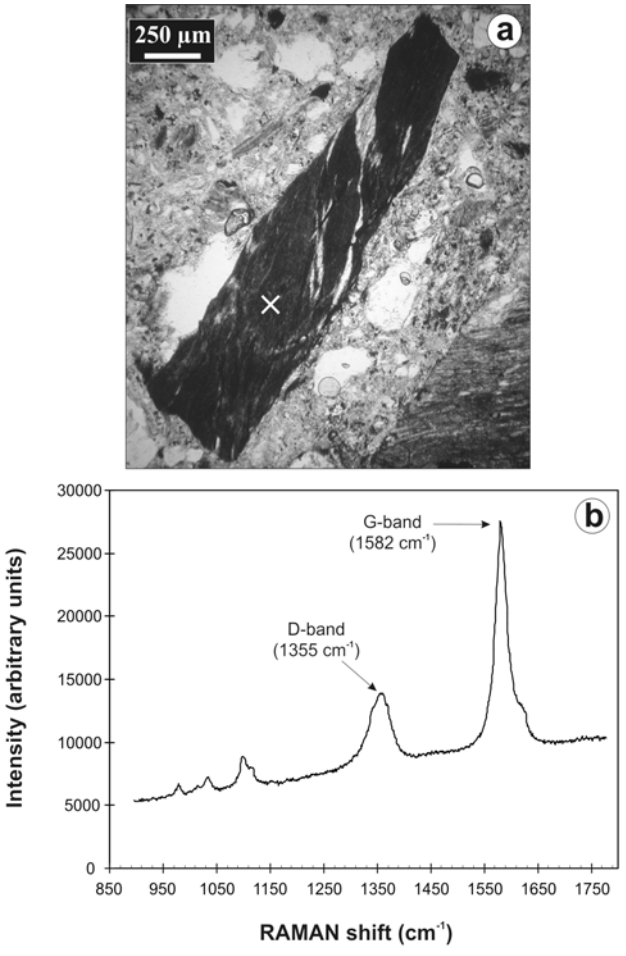

Fig. 5. a) A microphotograph of a carbon-rich shale clast in suevite (white cross indicates the area of the Raman spectroscopic measurement); sample KR8-004, depth = 239.65 m (plane-polarized light). b) A typical Raman spectrum from the carbon-rich shale clast, with one intrinsic band (G-band, 1582 cm^{-1}) originating from lattice vibration of graphite, and an additional defect-induced band (D-band, 1355 cm^{-1}). The intensity ratio between the G-band and the D-band is used to evaluate the structural ordering of carbonaceous matter (see Wopenka and Pasteris [1993] for more information).

Monomict meta-graywacke breccia is present at a depth between 310 and 311 m (Fig. 2) and is composed of meta-graywacke fragments (clast size from 1 to 10 cm) of variable grain size, from fine- to medium-grained. Only one sample from this monomict meta-graywacke breccia (KR8-049; depth = 310.23 m) was studied. It is locally sheared and, in order of decreasing abundance, is composed mainly of quartz, feldspar, muscovite, chlorite, epidote, sphene, and opaque minerals (pyrite and rutile). Aggregates of fine-grained calcite are abundant in the monomict meta-graywacke breccia.

We distinguish three units of a light greenish gray, medium-grained meta-graywacke that occur at 360.15, 421.6, and 445.8 m depth, at thicknesses of approximately 130, 85, and 195 cm, respectively (Fig. 2). These three units are concordant with the metasediment hosts and have been

Table 2a. Abundance of PDF sets in quartz grains from suevite samples (KR8-001, KR8-003, KR8-004, KR8-005, and KR8-006; depths = 235.77, 238.90, 239.65, 240.04, and 240.36 m, respectively).

Sets of planes	No. of grains	Percent (rel%)
1	28	34.2
2	43	52.4
3	7	8.5
4	4	4.9
151	82	100

151 planes were measured from 82 grains; plane /grain ratio (P/G = 1.70).

Table 2b. Abundance of PDF sets in quartz grains from meta-graywacke samples (KR8-029, KR8-030, KR8-031, and KR8-032; depths = 271.43, 272.00, 273.99, and 274.99 m, respectively).

Sets of planes	No. of grains	Percent (rel%)
1	24	40.7
2	29	49.1
3	5	8.5
4	1	1.7
101	59	100

101 planes were measured from 59 grains; plane /grain ratio (P/G = 1.71).

distinguished from the other meta-graywacke units (described before) by the characteristic light greenish gray color, easily discernible in hand specimen, and due to the abundance of chlorite. The first unit (at 360.15 m) is in part "pulverized" and more fractured than the two other units at depths of 421.6 and 445.8 m, which are rather less fractured. Some veinlets of quartz and calcite (up to 1 cm thick) are present with traces of pyrite in their interiors. At the microscopic scale, these light greenish gray, medium-grained meta-graywacke samples (KR8-069, KR8-106, KR8-121, and KR-122a; depths = 361.18, 421.88, 446.02, and 447.14 m, respectively) exhibit mainly (in order of decreasing abundance) feldspar, chloritoid, quartz, muscovite, sphene, and opaque minerals. Cuneiform intergrowths of quartz and feldspar (granophyric material) have been observed, and calcite in the form of local aggregates and/or pods is present. The four samples have the same mineral composition, but only one sample (KR8-069; depth = 361.18 m) contains quartz grains with PDFs (1 or 2 sets; some with a toasted appearance). This observation of shocked quartz grains was made on one sample (KR8-069) that was taken from the "pulverized" and strongly fractured unit at 361.18 m.

Phyllite and Slate: Phyllite and slate are gray to black in hand specimen, very fine- to fine-grained, well-banded, and folded (Fig. 14). Phyllite and slate are frequently associated and interbedded with fine- to medium-grained meta-graywacke in core (e.g., between 375 and 385 m) and hand specimen (e.g., KR8-109; depth = 425.24 m) (Fig. 12b), but also at the microscopic scale (e.g., KR8-063; depth = 343.57 m). Slate samples are more friable than phyllite samples.

These two lithologies are rare among our samples

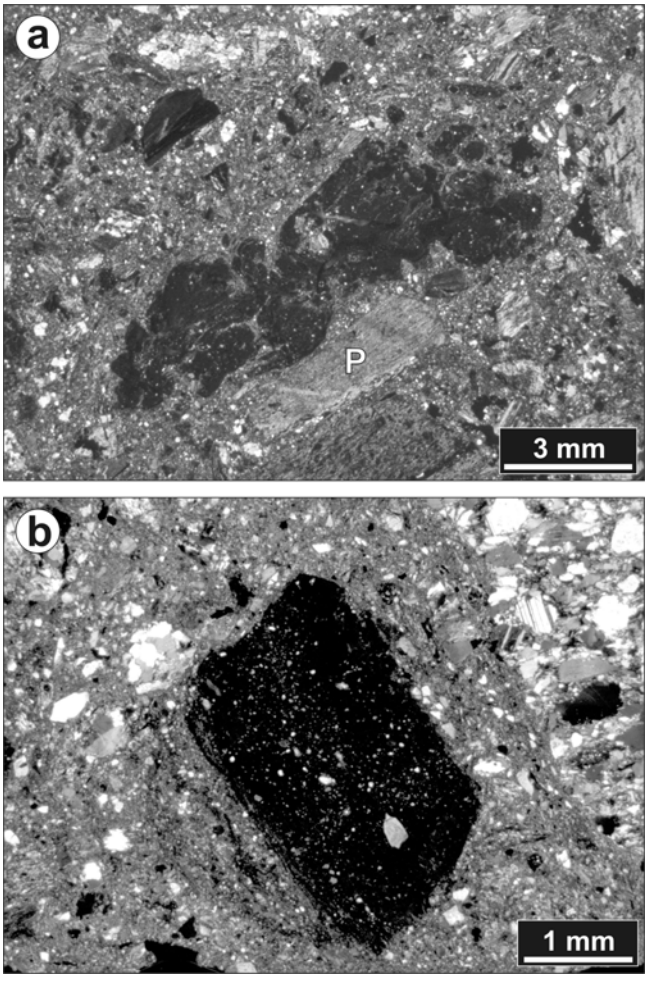

Fig. 6. Microphotographs (cross-polarized light) of melt particles in suevite. a) A mostly devitrified and irregular melt particle close to a phyllite clast (P). Sample KR8-004; depth = 239.65 m. b) A subangular melt particle (dark fragment) with small quartz clasts. Sample KR8-113; depth = 434.59 m.

(KR8-028, KR8-046, and KR8-063; depths = 266.18, 303.25, and 343.57 m, respectively) (Appendix 1). Microscopic observations on phyllite and slate samples showed that these two lithologies, in order of decreasing abundance, are mainly composed of mica (mainly muscovite and sericite) and quartz, with variable amounts of feldspar, chlorite, biotite, rutile, sphene, and pyrite. At the microscopic scale, minor fracturing frequently transects the rock; some of these microfractures are filled with iron oxides. Veinlets of granoblastic quartz, as well as primary calcite pods, are frequently observed. Shock metamorphic effects, mainly PFs but also some rare PDFs, have been observed in quartz grains from quartz veinlets that cross-cut phyllite and slate samples (e.g., KR8-063; depth = 343.57 m), which indicates that the veinlets predate the impact event.

Shock Petrographic Study: Basement rocks display a large heterogeneity of shock effects in quartz grains. The

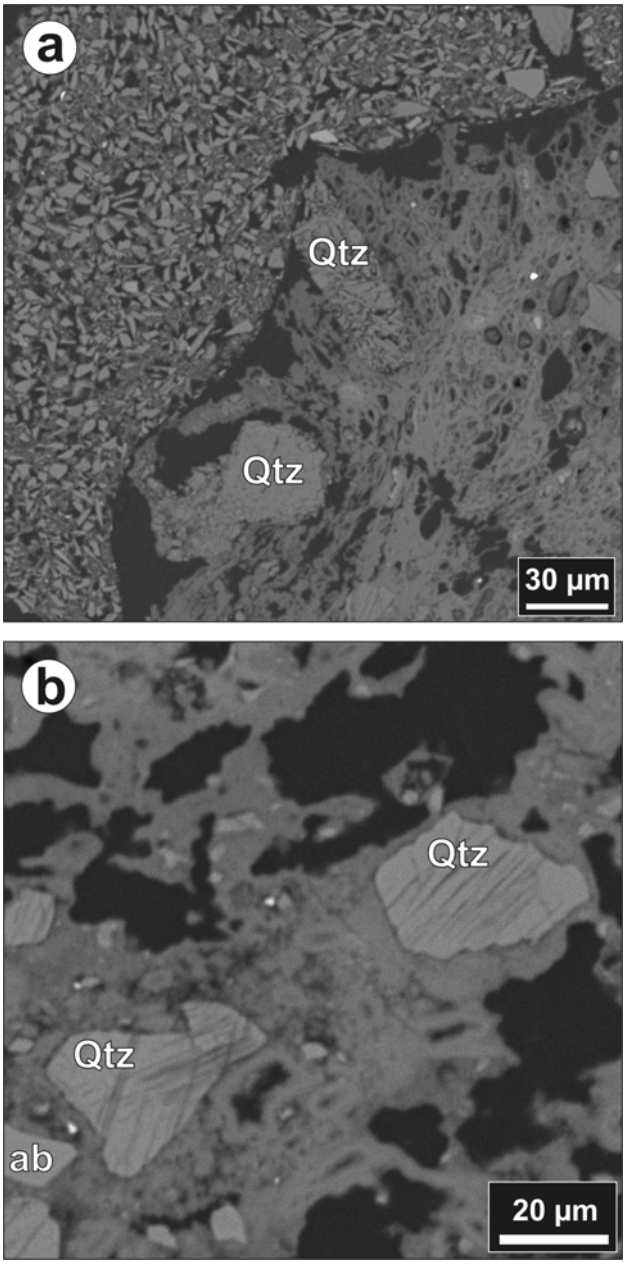

Fig. 7. Backscattered electron images showing the texture of two altered melt particles in suevite. a) Subangular lithic quartz grains in argillaceous matrix (left) and subrounded to subangular quartz grains embedded in argillaceous matrix (right). b) Shocked quartz grains embedded in argillaceous matrix with albite grains (ab); argillaceous matrix is dominated by illite. Sample KR8-004; depth = 239.65 m.

abundance of shocked quartz (with PFs and PDFs) in meta-graywacke samples is variable, from abundant (up to 38% of all quartz grains, in KR8-029 and KR8-032; depths = 271.43 and 274.99 m, respectively), many (up to 20%, in KR8-066 and KR8-067; depths = 353.95 and 356.59 m, respectively), to few (less than 5%) or not observed (for example, in KR8-125; depth = 451.23 m). See Appendix 1 for more detail. A detailed description of each sample allows us to

answer the question of the different response to shock effects for the different meta-graywacke samples (an apparent function of the grain size and of the relative abundances of quartz grains). Our observations revealed an apparent decrease of the number of shocked quartz grains with increasing depth. Even though meta-graywackes with similar grain sizes were used for this estimate, our conclusions need to be substantiated using a larger number of samples from more than three different depth intervals. Shocked quartz grains observed in meta-graywacke samples display PFs and PDFs (1, 2, or rarely 3 to 4 sets), some of which are decorated (Figs. 9b, 9c, and 9d). In some instances, the quartz grains are toasted (Figs. 9a and 9b). The crystallographic orientations of 155 PDF orientations in 89 quartz grains were analyzed on five thin sections of four meta-graywacke samples (KR8-029, KR8-030, KR8-031, and KR8-032; depths = 271.43, 272.00, 273.99, and 274.99 m, respectively) (Table 2b). More than 80% of all the poles to the PDF planes measured are oriented at ~23° to the c-axis (corresponding to the $\omega\{10\bar{1}3\}$ orientation). Less than 4% of planes parallel to the $\{22\bar{4}1\}$ orientation are present. Not more than 1% of the measured sets represent basal PDFs. The frequency of indexed PDF sets versus angle between c-axis and PDFs is shown in Fig. 10b.

Some feldspar grains display fractures or polysynthetic twinning displaced along microfaults; these features are preferentially observed in meta-graywacke, which also contains numerous shocked quartz grains (e.g., KR8-033; depth = 277.03 m). Several calcite grains show fractures, microfaults, and curved twins (e.g., KR8-108; depth = 424.78 m; Fig. 11b).

Suevite Dikelets

Suevite dikelets in metasediment occur between 279.5 and 298 m (three suevite dikelets of about 55 cm thickness at 280 m, 80 cm at 286 m, and 60 cm at 293.4 m), and between 418 and 440 m (three more suevite dikelets of about 35 cm thickness at 422.5 m, 65 cm at 434.3 m, and 60 cm at 440 m). In addition, thin suevite intercalations up to ~3 cm thick are present (e.g., at 418.05 m and around the suevite dikelet at 440 m) (Fig. 15). These suevite occurrences display a greenish gray, fine-grained fragmental matrix, consisting of rock and mineral fragments, and secondary smectite (mainly) and chlorite. Angular clasts of meta-graywacke, quartzite, phyllite, and slate occur. This greenish gray color of the suevite samples is due to the abundance of secondary phyllosilicates that results from the alteration of melt particles but also of matrix (Fig. 3d). Microscopic observations also reveal the presence of calcite fragments and of meta-graywacke clasts of the previously described "light greenish gray, medium-grained meta-graywacke" in suevite dikelet samples KR8-041, KR8-042, KR8-043, and KR8-107 from depths of 293.79, 293.97, 296.94, and 422.36 m, respectively.

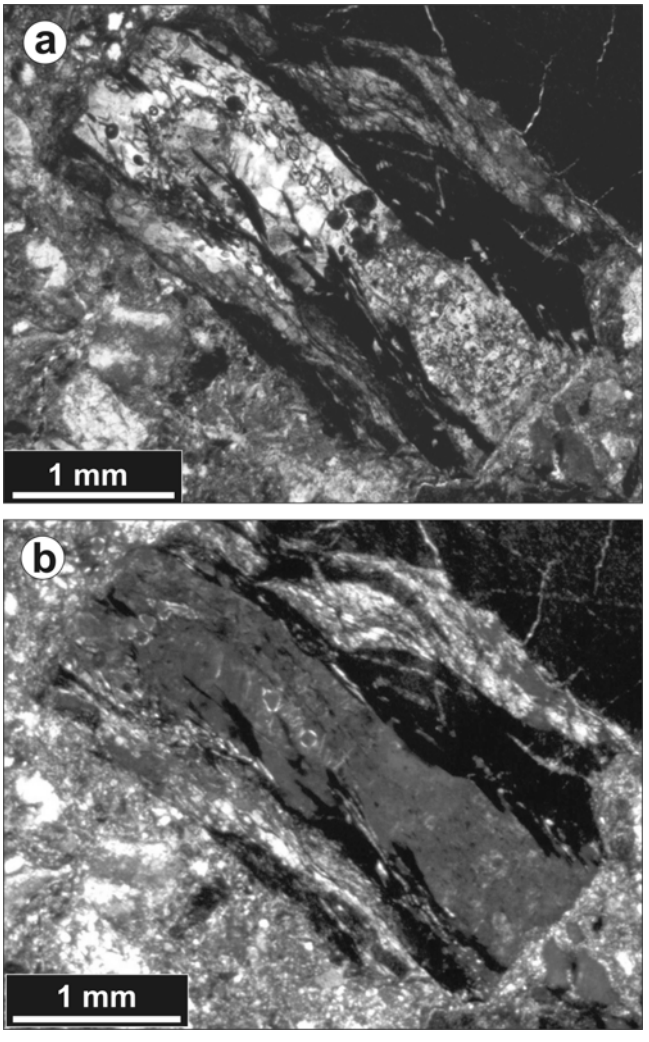

Fig. 8. A microphotograph of diaplectic quartz glass in suevite: (a) plane-polarized light and (b) cross-polarized light. Sample KR8-001; depth = 235.77 m.

Melt particles (Fig. 6b) are subangular to subrounded in shape and have sizes between 100 µm and 1 cm (in sample CAN-31, depth = 440.32 m). Melt particles present in suevite dikelets are mostly devitrified and altered to secondary phyllosilicates (Fig. 3d).

SUMMARY AND DISCUSSION

Core LB-08A can be subdivided into two major parts: the uppermost 25 m are composed of polymict lithic impact breccia (clast-supported) intercalated with suevite units (Fig. 2), and the lower part is composed of fractured/brecciated metasediment between 262 to 451 m, dominated by meta-graywacke (locally monomict lithic breccia), and intersected by a few suevite dikelets (Fig. 2). Because of the irregular distribution of melt particles in the upper 25 m of the core, the whole unit might be called a melt-poor suevite.

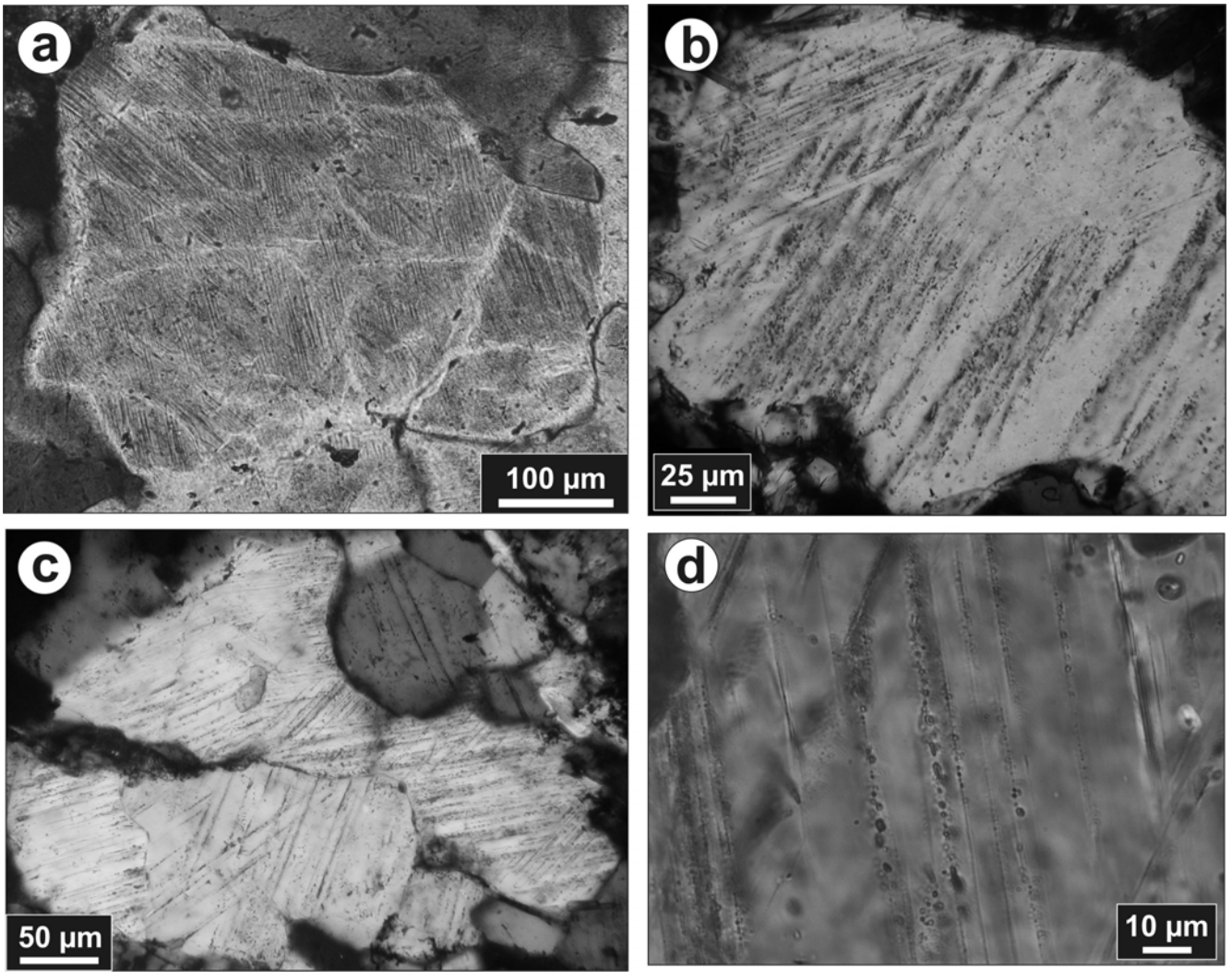

Fig. 9. Microphotographs in cross-polarized light. a) PDFs in quartz (locally toasted) from a quartzite clast in suevite. Sample KR8-006; depth = 240.36 m. b) Decorated PDFs in partially toasted quartz grains; medium-grained meta-graywacke. Sample KR8-056; depth = 326.78 m. c) Decorated PDFs in quartz grains; mylonitic medium-grained meta-graywacke. Sample KR8-070; depth = 364.12 m. d) Decorated (with numerous small fluid inclusions) PDFs in quartz grains; medium-grained meta-graywacke. Sample KR8-098; depth = 410.74 m.

However, our distinction between polymict lithic breccia and suevite is based on thin-section observations. This part of the core most likely represents fallback impact breccia. A deposition of this unit by slump processes is unlikely because after the formation of the crater—and even today—this location was topographically higher than the surrounding crater fill. Diaplectic quartz glass fragments are only present in the uppermost five meters of the core. It is not clear why diaplectic quartz glass fragments do not occur in all of the suevitic breccia parts of the fallback deposit.

The lower part of the core represents the basement that has been shocked and fractured during impact crater formation. The transition from impact breccia to basement is located at a depth of about 262 m below lake level. The basement is composed of an alternating sequence of metasediment with (in order of decreasing abundance) meta-graywacke (dominant), phyllite, and slate, with local occurrences of monomict lithic breccia, light greenish gray medium-grained meta-graywacke with granophyric material, and some suevite dikelets. The metasediment displays a large variation in lithology and grain size, from fine-grained to gritty, at the macroscopic and microscopic scales, which is normally typical of turbiditic deposits. The observations made during this study are in favor of a single structural unit; no major discontinuity has been observed in the lower part of the core.

The suevite dikelets observed in the metasediment (up to 80 cm thick; between 279.5 and 298 m, and between 418 and 440 m) are probably the result of injection of material into fractures. It is not clear whether, in addition to local fragments, material from all stratigraphic levels of the target was included in the suevite dikelets. However, the

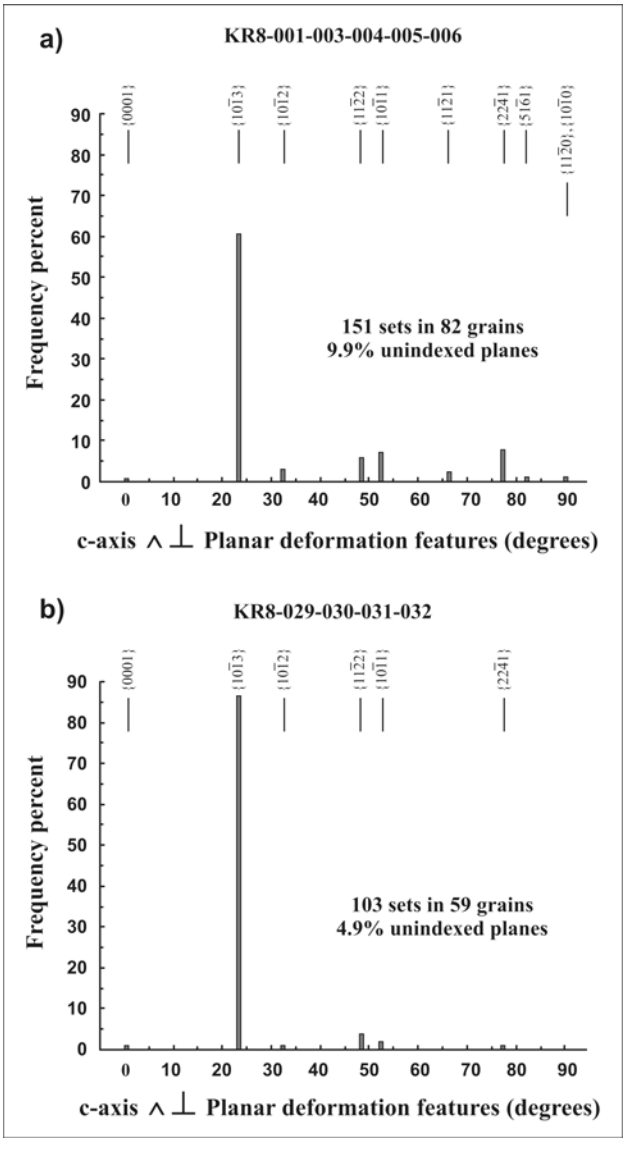

Fig. 10. Histograms of the frequency percent of uniquely indexed PDFs in quartz grains from (a) 5 suevite samples with depths between 235.77 and 240.36 m; and (b) 4 meta-graywacke samples from the basement with depths between 271.43 and 274.99 m. Note the very low frequency of basal (0001) PDFs. See text for details.

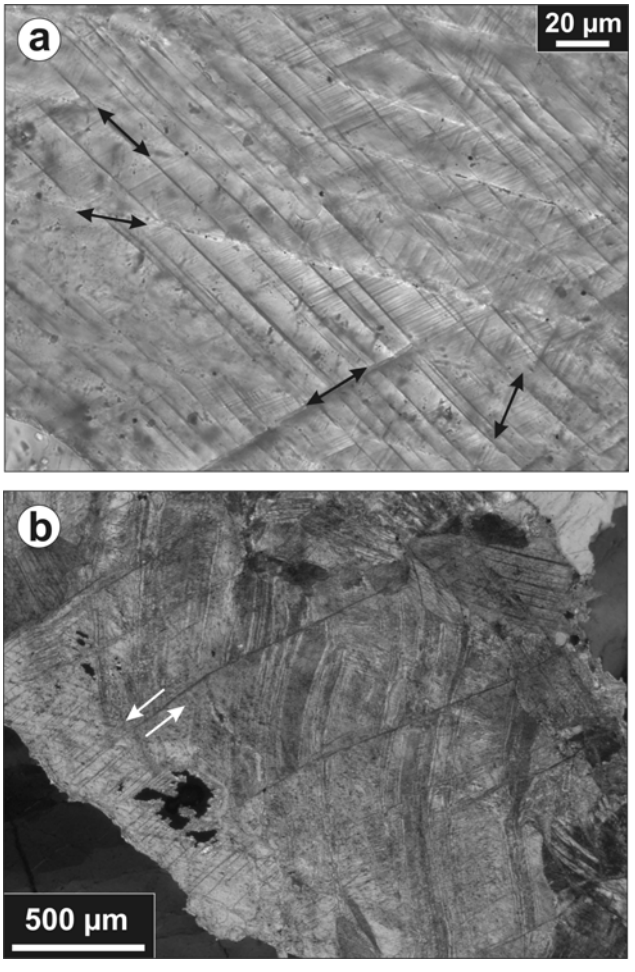

Fig. 11. Microphotographs of calcite grains. a) Grains with anomalous number of microfeatures (twins, cleavages, or planar fractures? Up to 4 different orientations). Suevite sample KR8-006; depth = 240.36 m (plane-polarized light). b) Grains with fractures, microfaults, and curved twins. Meta-graywacke sample KR8-108; depth = 424.78 m (cross-polarized light).

large variety of clast populations and presence of melt particles favors incorporation of material from the uppermost levels. It is also not clear whether the fractures into which the material was injected predate the impact event or were caused by it.

Shock Petrographic Characteristics of the Fallback Impact Breccia and of the Basement Samples, Drill Core LB-08A

Quartz grains with PFs and PDFs (commonly 1, 2, or 3 sets; rarely 4 sets) in suevite samples frequently display a toasted appearance (Short and Gold 1996; Whitehead et al. 2002). Some PDFs in quartz grains are decorated with numerous small fluid inclusions. Normally, decorated PDFs are considered secondary features, in which the decorations formed by post-shock annealing and aqueous alteration of non-decorated amorphous PDFs (e.g., Grieve et al. 1996; Leroux 2005). For this reason, the presence of decorated PDFs is surprising in the case of the Bosumtwi impact structure, which is only 1.07 Myr old. However, recent shock experiments (Kenkmann et al. 2006) show that it is possible to produce decorated PDFs in "wet" experiments (A. Deutsch and T. Kenkmann, personal communication), i.e., in experiments with target rocks saturated in water (Kenkmann et al. 2006). Observations of decorated PDFs in Bosumtwi samples argue for an impact into a water-rich metasedimentary target or, possibly, rapid post-impact alteration.

Orientations of PDF sets in quartz grains from suevite

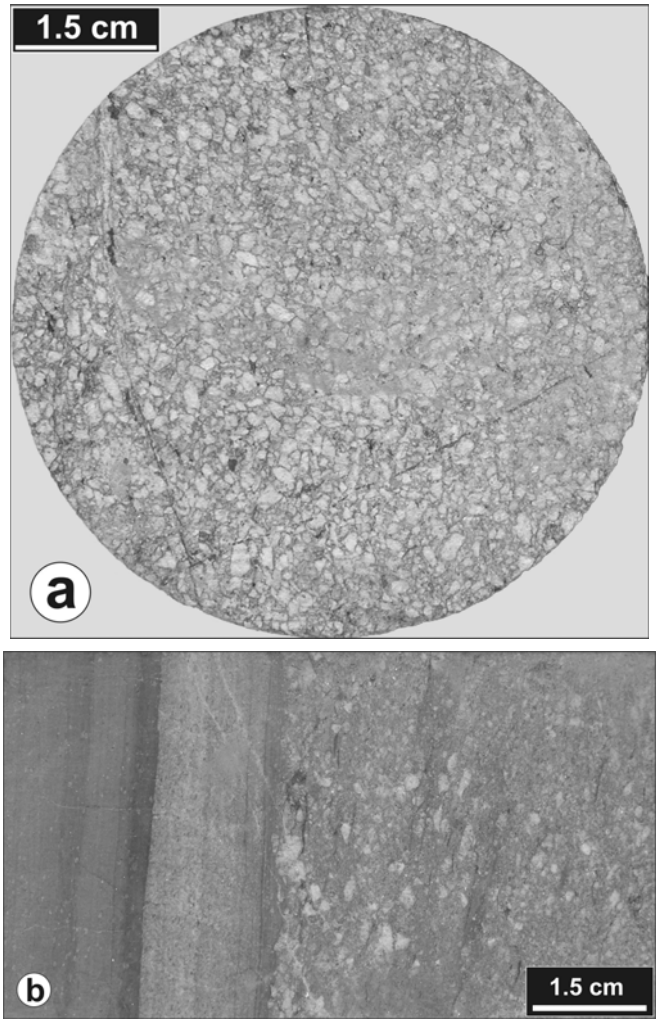

Fig. 12. Macrophotos. a) A core cross-section of gritty meta-graywacke. Sample KR8-029; depth = 271.43 m. b) Metasediment with large variation in grain size; from phyllite (left part), fine-grained meta-graywacke to medium-grained meta-graywacke (right part). Sample KR8-109; depth = 425.24 m.

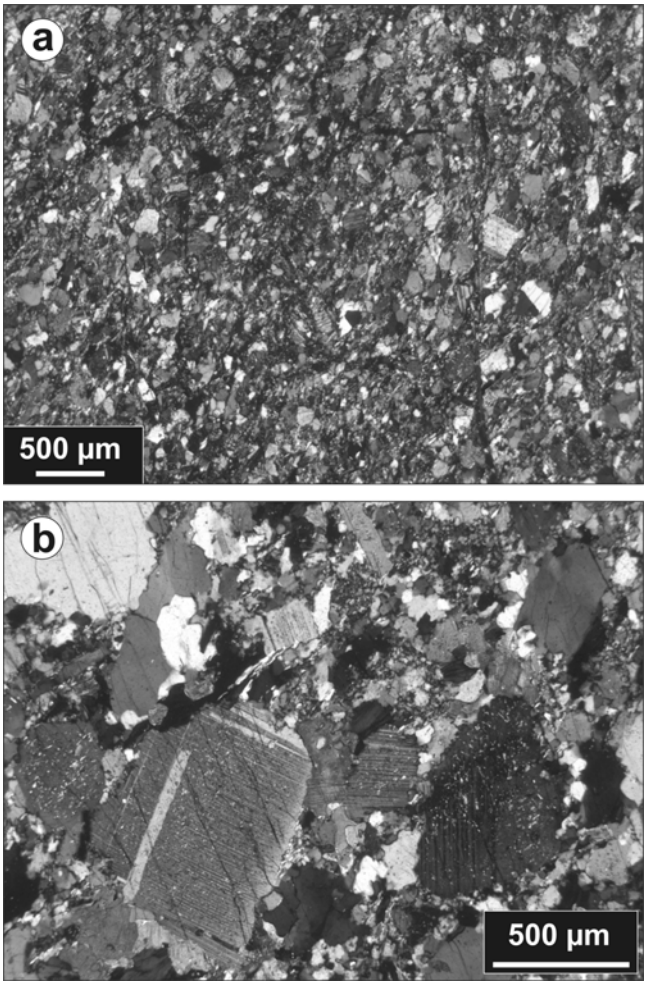

Fig. 13. Microphotographs (cross-polarized light). a) Sheared, fine-grained meta-graywacke cut by fine fractures. Sample KR8-027; depth = 263.76 m. b) Altered medium-grained to gritty meta-graywacke (partially annealed) with mainly fragments of feldspar and quartz. Sample KR8-123; depth = 447.96 m.

samples show that planes parallel to $\{10\bar{1}3\}$ are most abundant among the orientations of PDFs measured (up to 68 rel%) and that only a very small proportion of basal PDFs was found, which is in agreement with observations by Boamah and Koeberl (2006) on suevite from the northern outer sector of the impact structure. Such a frequency distribution of PDF orientations argues for shock pressures of at least 16 GPa (Grieve and Robertson 1976; Robertson et al. 1968; Huffman and Reimold 1996; French 1998), whereas shock pressures of up to 35 GPa in the top 5 m of the suevite are indicated by the presence of diaplectic quartz glass (e.g., Grieve et al. 1996), and the presence of melt particles in suevite indicates pressures higher than 45 GPa (e.g., French 1998). This heterogeneity of the shock levels in the suevite represents thorough mixing of variably shocked (and melted) target components.

Fractured and locally completely brecciated (presence of monomict meta-graywacke breccia; between 310 and 311 m) basement rocks display evidence of shock metamorphism, such as the presence of PFs and PDFs in quartz grains within meta-graywacke samples. The ratio of shocked to unshocked quartz grains in meta-graywacke seemingly decreases with depth, which can be related to shock pressure attenuation with distance from shock wave origin. On the basis of the different measurements of the poles to the PDF planes in quartz grains from meta-graywacke samples, largely dominated by planes parallel to $\{10\bar{1}3\}$ and low amount of planes parallel to $\{22\bar{4}1\}$, as well as the presence of up to 3 (or rarely 4) sets of PDFs in quartz grains, we have estimated that the intensity of shock pressure was highly heterogeneous in the basement, but shock pressures attained locally up to 25–30 GPa (Huffman and Reimold 1996; French 1998).

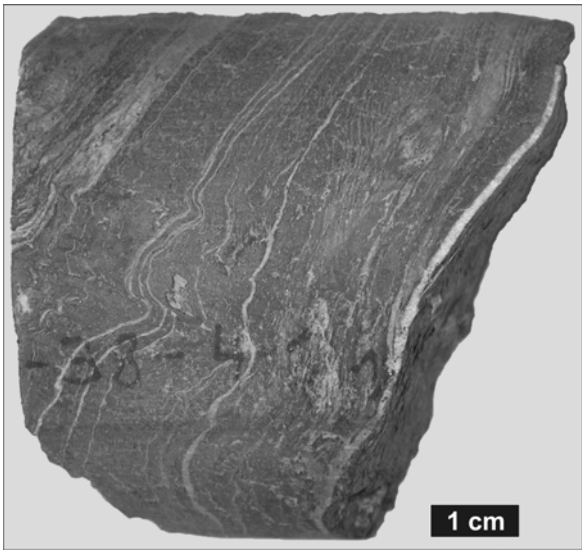

Fig. 14. A macrophoto of deformed phyllite with quartz laminae. Sample KR8-064; depth = 348.43 m.

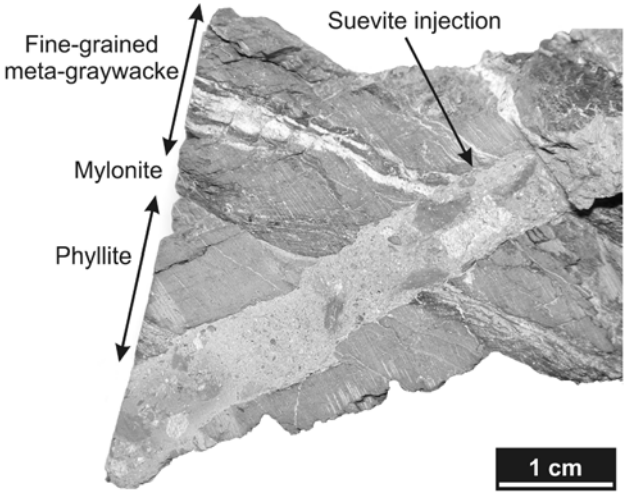

Fig. 15. A macrophoto of an altered suevite injection (~0.8 cm thick) in fine-grained metasediment (phyllite to fine-grained meta-graywacke, locally mylonitized and brecciated). Sample ADE-8A; depth = 418.05 m.

Alteration of the Rocks in Drill Core LB-08A

A variety of alteration effects has been observed in samples from the central uplift: alteration of plagioclase to sericite, biotite to chlorite, fractures filled with iron oxides, pyrite, and calcite veinlets and aggregates of secondary calcite. Alteration of plagioclase to sericite and biotite to chlorite took place mostly prior to the impact event, because rocks outside the crater show the same alteration features (Woodfield 1966; Moon and Mason 1967). Most of the fracture fills of iron oxides and pyrite flakes in the basement samples seem to be post-impact alteration features: the presence of calcite veinlets and aggregates in suevite samples from the fallback deposit indicates that they are secondary features likely resulting from hydrothermal circulation after the impact event (Kontny and Just 2006; Kontny et al. 2007). We have not observed by microscopic observation any systematic change in the distribution of calcite veinlets and aggregates with depth throughout the core, but CaO abundances measured in bulk samples (see Ferrière et al. 2007) show a weak trend of increasing abundances with depth. The majority of impact-melt particles in our fallback suevite samples, as well as in suevite dikelets in the basement, are devitrified and transformed to secondary phyllosilicates. The matrix of polymict impact breccia also contains an abundance of very fine-grained phyllosilicates, which is consistent with post-impact hydrothermal alteration.

Comparison with the Main Observations from Drill Core LB-07A

The LB-07A core, which was drilled into the deep crater moat, shows a number of differences compared to core LB-08A in terms of lithostratigraphy and also in terms of shock (Coney et al. 2007; Koeberl et al. 2007). In comparison with core LB-08A, which was subdivided into two major sections (this study), three sequences have been distinguished for the core LB-07A (Coney et al. 2007). The first 80 m of the core, termed “upper impactite” by Coney et al. (2007) (from 333.38 to 415.67 m in depth), consists of an alternating sequence of suevite and lithic impact breccias, underlain by the so-called “lower impactite,” which consists mostly of monomict lithic breccia (about 55 m), followed by the basement rocks (from 470.55 to 545.08 m in depth), and an assemblage of low-grade metapelites (including shale, schist, and phyllite), meta-graywacke, and minor meta-sandstone, quartzite, and thin carbonate strata (Coney et al. 2007).

These observations from core LB-07A indicate that at about 615 m to the northwest of the location of the core LB-08A, the thickness of the polymict impact breccia sequence is about three times greater. This major difference between the two cores could be the result of the transport during the crater modification stage, with material sliding off the top of the central uplift, or it could be the result of enhanced erosion of the top of the central uplift. The fact that the central part of the central uplift is collapsed (e.g., Scholz et al. 2002) indicates that some form of transport and material movement has taken place. The polymict lithic breccias in the upper sections of both cores may in fact represent debris flows off the central uplift and/or off the crater rim. This would explain the alternation of lithic breccia and suevite.

Concerning the occurrence of monomict impact breccia, just ~1 m of this lithology has been found in core LB-08A (this study) in comparison with ~55 m in core LB-07A (Coney et al. 2007). The basement underneath the crater seems to be heterogeneous, as metasediments observed in

core LB-07A are dominated by fine-grained rocks (mostly shale, schist, and phyllite) compared to the metasediments observed in the core LB-08A, which are mostly composed of fine- to medium-grained meta-graywacke. No gritty meta-graywacke has been observed in core LB-07A and, in turn, no shale and schist have been found in core LB-08A (this study; Deutsch et al. 2007).

In terms of shock petrography, both impactite sequences (in cores LB-07A and LB-08A) contain melt particles, which are more or less altered. Rare glass fragments have been found only in the top five meters of the fallback impact breccia in core LB-08A (this study), in comparison with the apparent absence of glass fragments in the upper impactite sequence in core LB-07A (Coney et al. 2007).

Comparison with Suevite from Outside the Crater

Melt particles and diaplectic quartz glass are present in suevite from the central uplift (Ferrière et al. 2006; this study), which is similar to suevites from outside the northern crater rim (Koeberl et al. 2002; Boamah and Koeberl 2003, 2006). However, melt particles and diaplectic quartz are rarer (about 6 vol%, with a maximum abundance of 10–15 vol% observed at the thin-section scale) and smaller (largest melt particle observed of ~1 cm) in suevite from the central uplift than in suevite from outside the northern crater rim; the abundance of impact-melt fragments in this suevite ranges from 15 vol% (Boamah and Koeberl 2003, 2006) to 60 vol% (Koeberl et al. 2002), and the size of the fragments is also up to more than ten times larger in suevite from outside the northern crater rim (up to 40 cm in diameter) (Koeberl and Reimold 2005). In addition, suevites from outside the crater rim contain coesite (Littler 1961), baddeleyite (the high-temperature decomposition product of zircon; El Goresy et al. 1968), and ballen quartz (Boamah and Koeberl 2003, 2006). Based on the presence of a sizable melt component in suevite from outside the crater rim and in suevite from the central uplift, shock pressures exceeding in both cases 45 GPa (according to Huffman and Reimold 1996; French 1998) can be assumed. However, it is clear that the relative amount of shocked and melted material in suevites from the central uplift is lower than in suevite from outside the northern crater rim.

Calcite clasts in suevite samples from the fallback deposit and also in suevite injected into the basement (also Coney et al. 2007) have not been observed before in polymict impact breccia from the Bosumtwi crater. Interestingly, we did not find any granite clasts in the suevite in core LB-08A, in contrast to suevite from outside the northern crater rim, which contains an up to 3 vol% component of granitic clasts (Boamah and Koeberl 2003, 2006; Koeberl et al. 2002).

The differences between suevite from the central uplift and suevite from outside the northern crater rim should represent differences in the ejection and deposition modes. To confirm these hypotheses, further detailed study of suevite deposits from the north side of the crater structure and of suevites from the occurrences to the south of the crater should be carried out.

Comparison with Observations at the Ries Impact Crater

Our observations of melt-particle abundance, i.e., lower melt-particle abundance in the fallback relative to the fallout breccia deposits, and distribution appear to be very similar to observations made at the Ries crater. Ries crater fallout suevite differs distinctly from the Ries fallback suevite with respect to volume, shape, and grain size of melt products and to volume and type of sedimentary rock inclusions, areal distribution, and thickness (Stöffler 1977; Stöffler et al. 1977).

Implications for Numerical Modeling

We have demonstrated in this study that the central uplift from Bosumtwi crater consists of fractured rocks, which are, at the location of borehole LB-08A, covered with about 25 m of polymict impact breccia. Neither in core LB-08A nor in core LB-07A (Coney et al. 2007) is there any significant amount of melt-rich suevite breccia or an indication of a coherent impact-melt lens, which was assumed to be present with a thickness of at least 200 m in the central part of the crater based on earlier geophysical and numerical modeling (Jones et al. 1981; Plado et al. 2000; Artemieva et al. 2004). The magnetic anomaly located in the northern part of the lake was previously interpreted to result from a melt-rich suevite layer (Jones et al. 1981; Plado et al. 2000), which has now been shown to be absent. How these observations compare with numerical investigations of tektite formation and deposition (Artemieva 2002) is not yet clear. Our study confirms that impact into metasedimentary target, especially into a wet metasedimentary target, produces only a limited amount of melt, which is widely and finely dispersed into the central part of the crater and under the form of large blobs outside of the crater rim. Whether or not oblique impact could have played a role is to be further investigated. Refined numerical modeling on the basis of these new observations may help to better understand the formation of the Bosumtwi crater.

CONCLUSIONS

The central uplift of the Bosumtwi impact structure was sampled for the first time during the 2004 ICDP drilling project, and here we present the first lithological, petrographic, mineralogical, and shock-petrographic observations on the rocks from drill core LB-08A. We have studied 174 thin sections by optical microscopy and 12 polished thin sections by electron microscopy from 121 samples covering the total depth range of the core, from 235.6 to 451.33 m below lake level.

Our main observations and conclusions are:

1. The uppermost 25 m of core LB-08A represent a fallback sequence containing melt particles, which indicates pressures >45 GPa, and diaplectic quartz glass, only observed in the top five meters, which indicates pressures of up to 35 GPa. The second part of the core, between 262 to 451 m, represents in situ heterogeneously shocked and fractured basement, with shock pressures locally reaching 25–30 GPa.
2. Melt particles and diaplectic quartz glass are rare in suevite from the central uplift in comparison with suevite samples from the northern part of the crater.
3. Observations of decorated PDFs in Bosumtwi samples argue for an impact into a water-bearing metasedimentary target or, possibly, rapid post-impact alteration.
4. The present study of samples from the central uplift, with comparison to observations on samples from outside the northern crater rim, yielded results that are concordant with observations from the Ries crater.

A more detailed optical and electron microscopic study of shocked minerals in all core units, as well as analyses of the proportion of shocked and unshocked quartz grains present in a variety of grain sizes from meta-graywacke samples and also of the relative abundance of quartz and feldspar grains throughout the basement, is in progress.

Acknowledgments–Drilling was funded by ICDP, the U.S. NSF, the Austrian FWF, the Canadian NSERC, and the Austrian Academy of Sciences. We are grateful to DOSECC for the drilling operations. This work was supported by the Austrian FWF (P17194-N10, to C. K.). We are grateful to F. Brandstätter (Natural History Museum, Vienna, Austria) and E. Robin (CEA, Gif-sur-Yvette, France) for assistance with electron microscopy and microprobe work, to J. N. Rouzaud and C. Le Guillou (both ENS, Paris, France) for assistance for Raman measurements, and to A. Deutsch and S. Luetke (both University of Muenster, Germany), and L. Coney and R. Gibson (University of the Witwatersrand, Johannesburg, South Africa) for constructive discussions. We are grateful to J. Morrow and D. Kring for constructive reviews.

Editorial Handling—Dr. Bernd Milkereit

REFERENCES

Artemieva N. A. 2002. Tektite origin in oblique impact: Numerical modeling. In *Impacts in Precambrian shields*, edited by Plado J. and Pesonen L. New York: Springer-Verlag. pp. 257–276.

Artemieva N. A., Karp T., and Milkereit B. 2004. Investigating the Lake Bosumtwi impact structure: Insight from numerical modeling. *Geochemistry Geophysics Geosystems* 5, doi:10.1029/2004GC000733.

Boamah D. and Koeberl C. 2003. Geology and geochemistry of shallow drill cores from the Bosumtwi impact structure, Ghana. *Meteoritics & Planetary Science* 38:1137–1159.

Boamah D. and Koeberl C. 2006. Petrographic studies of fallout suevite from outside the Bosumtwi impact structure, Ghana. *Meteoritics & Planetary Science* 41:1761–1774.

Brodie K., Fettes D., Harte B., and Schmid R. 2004. Structural terms including fault rock terms. http://www.bgs.ac.uk/scmr/docs/paper_3/scmr_struc2.pdf.

Chayes F. 1949. A simple point counter for thin-section analysis. *American Mineralogist* 34:1–11.

Coney L., Reimold W. U., Koeberl C., and Gibson R. L. 2006. Mineralogical and geochemical investigations of impact breccias in the ICDP borehole LB-07A, Bosumtwi impact structure, Ghana (abstract #1279). 37th Lunar and Planetary Science Conference. CD-ROM.

Coney L., Gibson R. L., Reimold W. U., and Koeberl C. 2007. Lithostratigraphic and petrographic analysis of ICDP drill core LB-07A, Bosumtwi impact structure, Ghana. *Meteoritics & Planetary Science* 42. This issue.

Deutsch A., Luetke S., and Heinrich V. 2007. The ICDP Lake Bosumtwi impact crater scientific drilling project (Ghana): Core LB-08A litho-log, related ejecta, and shock recovery experiments. *Meteoritics & Planetary Science* 42. This issue.

El Goresy A., Fechtig H., and Ottemann T. 1968. The opaque minerals in impactite glasses. In *Shock metamorphism of natural materials*, edited by French B. M. and Short N. M. Baltimore: Mono Book Corp. pp. 531–554.

Emmons R. C. 1943. *The universal stage (with five axes of rotation)*. GSA Memoir #8. New York: Geological Society of America. 205 p.

Engelhardt W. von and Bertsch W. 1969. Shock-induced planar deformation structures in quartz from the Ries crater, Germany. *Contributions to Mineralogy and Petrology* 20:203–234.

Ferrière L., Koeberl C., Reimold W. U., and Gibson R. L. 2006. First mineralogical observations and chemical analyses of core LB-08A from the central uplift of the Bosumtwi impact structure, Ghana: Comparison with suevite from outside the crater (abstract #1845). 37th Lunar and Planetary Science Conference. CD-ROM.

Ferrière L., Koeberl C., Reimold W. U., and Mader D. 2007. Drill core LB-08A, Bosumtwi impact structure, Ghana: Geochemistry of fallback breccia and basement samples from the central uplift. *Meteoritics & Planetary Science* 42. This issue.

French B. M. 1998. *Traces of catastrophe: A handbook of shock-metamorphic effects in terrestrial meteorite impact structures*. LPI Contribution #954. Houston: Lunar and Planetary Institute. 120 p.

Grieve R. A. F. and Robertson P. B. 1976. Variations in shock deformation at the Slate Islands impact structure, Lake Superior, Canada. *Contributions to Mineralogy and Petrology* 58:37–49.

Grieve R. A. F., Langenhorst F., and Stöffler D. 1996. Shock metamorphism of quartz in nature and experiment: II. Significance in geoscience. *Meteoritics & Planetary Science* 31: 6–35.

Huffman A. R. and Reimold W. U. 1996. Experimental constraints on shock-induced microstructures in naturally deformed silicates. *Tectonophysics* 256:165–217.

Jackson J. A. 1997. *Glossary of geology,* 4th ed. Alexandria, Virginia: American Geological Institute. 769 p.

Jones W. B., Bacon M., and Hastings D. A. 1981. The Lake Bosumtwi impact crater, Ghana. *Geological Society of America Bulletin* 92:342–349.

Junner N. R. 1937. The geology of the Bosumtwi caldera and surrounding country. *Gold Coast Geological Survey Bulletin* 8: 1–38.

Karp T., Milkereit B., Janle P., Danuor S. K., Pohl J., Berckhemer H., and Scholz C. A. 2002. Seismic investigation of the Lake Bosumtwi impact crater: Preliminary results. *Planetary and Space Science* 50:735–742.

Kenkmann T., Thoma K., and the MEMIN team 2006. Hypervelocity impact into dry and wet sandstone (abstract). *Geophysical Research Abstracts* 8:A-02389.

Koeberl C. and Reimold W. U. 2005. Bosumtwi impact crater, Ghana (West Africa): An updated and revised geological map, with explanations. *Jahrbuch der Geologischen Bundesanstalt, Wien* (Yearbook of the Austrian Geological Survey). 145:31–70 (+1 map, 1:50,000).

Koeberl C., Bottomley R. J., Glass B. P., and Storzer D. 1997. Geochemistry and age of Ivory Coast tektites and microtektites. *Geochimica et Cosmochimica Acta* 61:1745–1772.

Koeberl C., Reimold W. U., Blum J. D., and Chamberlain C. P. 1998. Petrology and geochemistry of target rocks from the Bosumtwi impact structure, Ghana, and comparison with Ivory Coast tektites. *Geochimica et Cosmochimica Acta* 62:2179–2196.

Koeberl C., Denison C., Ketcham R. A., and Reimold W. U. 2002. High-resolution X-ray computed tomography of impactites. *Journal of Geophysical Research* 107, doi:10.1029/2001JE001833.

Koeberl C., Milkereit B., Overpeck J. T., Scholz C. A., Reimold W. U., Amoako P. Y. O., Boamah D., Claeys P., Danuor S. K., Deutsch A., Hecky R. E., King J., Newsom H., Peck J., and Schmitt D. R. 2006. An international and multidisciplinary drilling project into a young complex impact structure: The 2004 ICDP Bosumtwi impact crater, Ghana, drilling project—An overview (abstract #1859). 37th Lunar and Planetary Science Conference. CD-ROM.

Koeberl C., Milkereit B., Overpeck J. T., Scholz C. A., Amoako P. Y. O., Boamah D., Danuor S., Karp T., Kueck J., Hecky R. E., King J. W., and Peck J. A. 2007. An international and multidisciplinary drilling project into a young complex impact structure. The 2004 ICDP Bosumtwi Crater Drilling Project—An overview. *Meteoritics & Planetary Science* 42. This issue.

Kontny A. and Just J. 2006. Magnetic mineralogy and rock magnetic properties of impact breccias and crystalline basement rocks from the BCDP-drillings 7A and 8A (abstract #1343). 37th Lunar and Planetary Science Conference. CD-ROM.

Kontny A., Elbra T., Just J., Pesonen L. J., Schleicher A., and Zolk J. 2007. Petrography and shock-related remagnetization of pyrrhotite in drill cores from the Bosumtwi Crater Drilling Project, Ghana. *Meteoritics & Planetary Science* 42. This issue.

Langenhorst F. 2002. Shock metamorphism of some minerals: Basic introduction and microstructural observations. *Bulletin of the Czech Geological Survey* 77:265–282.

Leroux H. 2005. Weathering features in shocked quartz from the Ries impact crater, Germany. *Meteoritics & Planetary Science* 40: 1347–1352.

Leube A., Hirdes W., Mauer R., and Kesse G. O. 1990. The Early Proterozoic Birimian Supergroup of Ghana and some aspects of its associated gold mineralization. *Precambrian Research* 46: 139–165.

Littler J., Fahey J. J., Dietz R. S., and Chao E. C. T. 1961. Coesite from the Lake Bosumtwi crater, Ashanti, Ghana. GSA Special Paper #68. Boulder, Colorado: Geological Society of America. 218 p.

Montanari A. and Koeberl C. 2000. *Impact stratigraphy: The Italian record*. Lecture Notes in Earth Sciences, vol. 93. Heidelberg: Springer-Verlag. 364 p.

Moon P. A. and Mason D. 1967. The geology of ¼° field sheets 129 and 131, Bompata S. W. and N. W. *Ghana Geological Survey Bulletin* 31:1–51.

Pesonen L. J., Koeberl C., Ojamo H., Hautaniemi H., Elo S., and Plado J. 1998. Aerogeophysical studies of the Bosumtwi impact structure, Ghana (abstract). *Geological Society of America Abstracts with Programs* 30:A190.

Pesonen L. J., Koeberl C., and Hautaniemi H. 2003. Airborne geophysical survey of the Lake Bosumtwi meteorite impact structure (southern Ghana)—Geophysical maps with descriptions. *Jahrbuch der Geologischen Bundesanstalt, Vienna (Yearbook of the Austrian Geological Survey)* 143:581–604.

Plado J., Pesonen L. J., Koeberl C., and Elo S. 2000. The Bosumtwi meteorite impact structure, Ghana: A magnetic model. *Meteoritics & Planetary Science* 35:723–732.

Reimold W. U., Brandt D., and Koeberl C. 1998. Detailed structural analysis of the rim of a large, complex impact crater: Bosumtwi crater, Ghana. *Geology* 26:543–546.

Reinhard M. 1931. *Universaldrehtischmethoden*. Basel, Switzerland: Birkhäuser. 118 p.

Robertson P. B., Dence M. R., and Vos M. A. 1968. Deformation in rock-forming minerals from Canadian craters. In S*hock metamorphism of natural materials*, edited by French B. M. and Short N. M. Baltimore: Mono Book Corp. pp. 433–452.

Scholz C. A., Karp T., Brooks K. M., Milkereit B., Amoako P. Y. O., and Arko J. A. 2002. Pronounced central uplift identified in the Bosumtwi impact structure, Ghana, using multichannel seismic reflection data. *Geology* 30:939–942.

Short N. M. and Gold D. P. 1996. Petrography of shocked rocks from the central peak at the Manson impact structure. GSA Special Paper #302. Boulder, Colorado: Geological Society of America. pp. 245–265.

Stöffler D. 1977. Research drilling Nördlingen 1973: Polymict breccias, crater basement, and cratering model of the Ries impact structure. *Geologica Bavarica* 75:443–458.

Stöffler D. and Grieve R. A. F. 1994. Classification and nomenclature of impact metamorphic rocks: A proposal to the IUGS subcommission on the systematics of metamorphic rocks. In *ESF Scientific Network on Impact Cratering and Evolution of Planet Earth, Post-Östersund Newsletter*, edited by Montanari A. and Smit J. pp. 9–15.

Stöffler D. and Langenhorst F. 1994. Shock metamorphism of quartz in nature and experiment: I. Basic observation and theory. *Meteoritics* 29:155–181.

Stöffler D., Ewald U., Ostertag R., and Reimold W. U. 1977. Research drilling Nördlingen 1973 (Ries): Composition and texture of polymict breccias. *Geologica Bavarica* 75:163–189.

Whitehead J., Spray J. G., and Grieve R. A. F. 2002. Origin of "toasted" quartz in terrestrial impact structures. *Geology* 30:431–434.

Wopenka B. and Pasteris J. D. 1993. Structural characterization of kerogens to granulites-facies graphite: Applicability of Raman spectroscopy. *American Mineralogist* 78:533–577.

Woodfield P. D. 1966. The geology of the ¼° field sheet 91, Fumso N. W. *Ghana Geological Survey Bulletin* 30:1–66.

Wright J. B., Hastings D. A., Jones W. B., and Williams H. R. 1985. *Geology and mineral resources of West Africa*. London: Allen & Unwin. 187 p.

APPENDIX

Appendix 1. Detailed petrographic descriptions (rock name, minerals present, etc.) and depths of the 121 samples documented for this study. This table is based on optical microscopic observations of 174 thin sections.

Sample no.	Depth (m)	Petrographic description
KR8-001	235.77	Suevite with a variety of lithic and mineral clasts: meta-graywacke, phyllite, slate, melt particles (partially or completely devitrified), carbon-rich organic shale, diaplectic quartz glass, and calcite; quartz grains show some PFs and PDFs (1 or 2 sets; one quartz grains with 3 sets)
KR8-002	236.40	Phyllite (clast) with quartzitic laminae/ribbon quartz; local development of crenulation cleavage; no obvious shock effects; similar to KR8-007
KR8-003	238.90	Suevite; very similar to KR8-001 in composition and appearance (but no diaplectic quartz glass seen); a few quartz grains with 1 or 2 sets of PDFs
KR8-004	239.65	Suevite with a variety of lithic and mineral clasts: phyllite and slate, mylonitic meta-graywacke, quartzite, melt particles (in a few cases with flow structure and vesicles), and carbon-rich organic shale clasts (few in comparison with KR8-001 and KR8-003); many melt particles (one large one, ~1 cm in the longest dimension); some quartz grains with PDFs (1 or 2 sets); fractures filled with iron oxides and calcite aggregates
KR8-005	240.04	Suevite with a variety of lithic and mineral clasts: phyllite (similar to KR8-002, with large ribbon quartz) and slate, melt particles (brown or black in color and with vesicles), mylonitic meta-graywacke, carbon-rich organic shale, quartzite, calcite, and diaplectic quartz glass; quartz grains show some PFs and PDFs (1 or 2 sets; one quartz grains with 3 sets)
KR8-006	240.36	Quartzite clast in suevite; plenty of PDFs (1, 2, 3, and 4 sets) in quartz grains partially or totally toasted; presence of cracks filled by calcite; a small part of the section comprises suevite
KR8-007	241.94	Phyllite (clast) with quartzitic laminae/ribbon quartz; presence of chlorite veinlets (aligned parallel to the foliation); no trace of shock deformation; very similar to KR8-002
KR8-008	244.45	Strongly altered polymict lithic breccia (clasts supported) with a variety of clasts: meta-graywacke (some mylonitic), phyllite and slate, and quartzite
KR8-009	244.87	Altered polymict lithic breccia (clast supported); faulted clasts of phyllite and slate with quartzitic beds and breccia veins (matrix-poor); phyllite and slate (dominant), quartzite, meta-graywacke (minor) clasts; some of the quartz grains show undulatory extinction and few PFs and PDFs (1 or 2 sets)
KR8-010	245.58	Altered polymict lithic breccia with injected suevitic breccia (vein)
KR8-011	247.46	Altered polymict lithic breccia; composed mainly of mylonitic meta-graywacke, quartzite, and phyllite and slate clasts; many PFs and PDFs (1 or 2 sets, one grain with 3 sets) in quartz grains; calcite aggregates occur
KR8-012	248.00	Suevite with a variety of clasts: mylonitic meta-graywacke, phyllite and slate (fine-grained, well-foliated and with locally development of crenulation cleavage), melt particles (devitrified), quartzite, and carbon-rich organic shale and calcite (minor); some calcite aggregates occur
KR8-013	248.80	Altered polymict lithic breccia; composed mainly of mylonitic meta-graywacke, quartzite, and phyllite and slate clasts; many PFs and PDFs (1 or 2 sets) in quartz grains (locally toasted); calcite aggregates and elongated opaque crystals occur; similar to KR8-011
KR8-014	249.30	Suevite (matrix dominate) with a variety of lithic and mineral clasts: altered meta-graywacke, phyllite and slate, melt particles (gray to brown in color), quartzite, and calcite; few PFs and PDFs with 1 set (only 3 quartz grains with 2 sets of PDFs each)
KR8-015	250.74	Altered polymict lithic breccia (clasts supported); composed of two different clast types, phyllite (and slate) and mylonitic meta-graywacke; lots of the quartz grains are fractured, a few show undulatory extinction, and a few others PFs and PDFs (1 or 2 sets)
KR8-016	250.89	Strongly altered polymict lithic breccia with injected suevitic breccia (veinlet); composed of a variety of clasts: phyllite and slate (with development of crenulation cleavage), mylonitic meta-graywacke, melt particles (brown in color) that are completely devitrified, and quartzite; alteration mainly around the suevitic breccia veinlet
KR8-017	251.74	Altered polymict lithic breccia (clasts supported); composed of two different clast types, phyllite (and slate) and mylonitic meta-graywacke; some of the quartz grains show cracks, PFs, and PDFs (1 or 2 sets); very similar to KR8-015
KR8-018	253.04	Altered polymict lithic breccia (clast-supported); composed of two different clast types, phyllite (and slate) and mylonitic meta-graywacke; aggregates of small opaque minerals and tabular opaque crystals occur; few calcite aggregates; very similar to KR8-015 and KR8-017
KR8-019	253.56	Altered polymict lithic breccia with injected suevitic breccia veinlets; composed of meta-graywacke clasts (dominant), few melt particles (altered), phyllite and slate, and calcite clasts; very few PFs (no PDFs seen); abundant calcite aggregates and veinlets
KR8-021	255.65	Altered polymict lithic breccia (clast-supported); few quartz grains show PFs (no PDFs seen); many calcite aggregates and veinlets; very similar to KR8-015, KR8-017, and KR8-018
KR8-022	256.81	Altered polymict lithic breccia (clast-supported); presence of a tiny suevitic veinlet mostly composed of melt particles, isotropic quartz grains, and quartz grains with undulatory extinction); many calcite aggregates and veinlets; no PDFs seen; sample very similar to KR8-015, KR8-017, KR8-018, and KR8-021

Appendix 1. *Continued.* Detailed petrographic descriptions (rock name, minerals present, etc.) and depths of the 121 samples documented for this study. This table is based on optical microscopic observations of 174 thin sections.

Sample no.	Depth (m)	Petrographic description
KR8-023	258.14	Suevite with a variety of clasts: meta-graywacke (medium-grained meta-graywacke dominant) to mylonitic meta-graywacke, slate and phyllite, melt particles (brown in color), quartzite, and minor calcite; few quartz grains (some partially toasted) show PFs (no PDFs seen); a few feldspar crystals are recrystallized (myrmekitic intergrowths of quartz and feldspar)
KR8-024	259.14	Altered polymict lithic breccia (clast-supported); composed of two different clast types, mylonitic meta-graywacke as well as faulted phyllite (and slate); unusual outline (step-like; possibly result of faulting) of phyllite in contact with mylonitic meta-graywacke; very few quartz grains show PFs (no PDFs seen); fine-grained breccia veinlets (suevite?); many opaque grains
KR8-025	259.74	Suevite with a variety of clasts: meta-graywacke (fine- to medium-grained; some are mylonitic or sheared), quartzite, slate, phyllite, melt particles brown to black in color, and few calcite clasts; very few quartz grains with PFs (no PDFs seen); some calcite and opaque minerals aggregates occur
KR8-026	260.49	Suevite with a variety of lithic and mineral clasts: phyllite, fine- to medium-grained meta-graywacke (some are mylonitic), melt particles (brown or black in color), quartzite, slate, and calcite; many quartz grains show PDFs (1 or 2 sets), generally decorated, and some quartz grains are partially toasted; a few feldspar crystals are recrystallized with spherulitic texture (myrmekitic intergrowths of quartz and feldspar); large opaque minerals (pyrite)
KR8-027	263.76	Sheared, fine-grained meta-graywacke; some quartz grains show PFs and PDFs (few grains with 2 sets of PDFs each); calcite veins, veinlets, and aggregates occur
KR8-028	266.18	Very fine-grained metasediment (slate); a few PDFs in quartz (1 set); opaque minerals (pyrite) occur; sample very similar to KR8-046
KR8-029	271.43	Gritty meta-graywacke; plenty of PDFs in quartz (1, 2, or rarely 3 sets; one grain with 4 sets)
KR8-030	272.00	Gritty meta-graywacke; plenty of PDFs in quartz (1 or 2 sets); very similar to KR8-029
KR8-031	273.99	Gritty meta-graywacke; plenty of PDFs in quartz (1, 2, or rarely 3 sets)
KR8-032	274.99	Medium-grained to gritty meta-graywacke; plenty of PDFs (1, 2, or 3 sets) in quartz grains that are partially toasted
KR8-033	277.03	Medium-grained meta-graywacke; lots of PDFs in quartz (1 or 2 sets), some are decorated, and some partially toasted; shock-induced twinning in plagioclase
KR8-034	277.89	Mylonitic, medium-grained to gritty meta-graywacke (locally brecciated); lots of PDFs in quartz (1 or 2 sets), some decorated, and some grains are partially toasted
KR8-035	280.30	Altered suevite with a variety of lithic and mineral clasts: meta-graywacke (sheared or mylonitic), quartzite, phyllite and slate (some clasts displays crenulation cleavage), altered melt particles (gray to brown in color), and calcite clasts; quartz grains show cracks, some grains display PDFs (1 or 2 sets), and a few are toasted
KR8-036	281.32	Mylonitic, medium-grained meta-graywacke; abundant PDFs in quartz (1 or 2 sets); some quartz grains are partially toasted
KR8-037	283.50	Mylonitic, medium-grained meta-graywacke; many PDFs in quartz (1 or 2 sets)
KR8-038	283.74	Brecciated meta-graywacke locally mylonized; lots of PDFs in quartz (1 or 2 sets); some quartz grains are partially toasted
KR8-039	286.17	Strongly altered suevite with a variety of lithic and mineral clasts: abundant melt particles (gray to brown in color), meta-graywacke (some mylonitic), quartzite, phyllite and slate, and calcite clasts
KR8-040	290.47	Suevite with a variety of lithic and mineral clasts: meta-graywacke clast (altered, weakly sheared fine-grained meta-graywacke principally), phyllite, melt particles (mostly brown in color), and calcite; only very few quartz grains display PFs (only one grain with 1 set of PDFs)
KR8-041	293.79	Suevite with a variety of lithic and mineral clasts: phyllite, slate, shocked medium-grained meta-graywacke, chloritoid-rich meta-graywacke, melt particles (brown in color), quartzite, and calcite clasts; a few quartz grains show PFs or PDFs (1 set)
KR8-042	293.97	Suevite (with a prominent phyllite clast) with a variety of lithic and mineral clasts: phyllite and slate, meta-graywacke (mainly mylonitic and some chloritoid-rich meta-graywacke), brown melt particles, quartzite, and calcite
KR8-043	296.94	Strongly altered suevite with a variety of lithic and mineral clasts: phyllite and slate, meta-graywacke (mylonitic, fine- to medium-grained meta-graywacke and some chloritoid-rich meta-graywacke), melt particles (brown in color), quartzite, and calcite; a few quartz grains with PDFs (1 or 2 sets)
KR8-045	300.41	Weakly sheared, heterogranular meta-graywacke (fine- to medium-grained); quartz grains show cracks and some are partially isotropic; some quartz grains with PDFs, generally decorated (1 or 2 sets), and some grains are partially toasted; a few quartz grains display broad, sometimes planar fluid inclusion trails
KR8-046	303.25	Very fine-grained slate; a small quartz veinlet with few quartz grains with PFs and PDFs; sample very similar to KR8-028
KR8-047	305.71	Alternating slate and sheared, fine-grained meta-graywacke; quartz grains show fracturing, some PFs, and a few PDFs (1 set) that are generally decorated
KR8-048	307.30	Altered protomylonitic medium-grained meta-graywacke, locally cataclastic; few PFs and PDFs; allanite and zircon occur; numerous penetrative fractures filled by iron oxides and/or by chlorite; presence of calcite aggregates

Appendix 1. *Continued.* Detailed petrographic descriptions (rock name, minerals present, etc.) and depths of the 121 samples documented for this study. This table is based on optical microscopic observations of 174 thin sections.

Sample no.	Depth (m)	Petrographic description
KR8-049	310.23	Medium-grained meta-graywacke breccia, locally sheared or cataclastic; some PFs and a few PDFs (1 set); many calcite aggregates occur
KR8-050	310.99	Heterogranular meta-graywacke; few PFs (no PDFs seen) in quartz grains; abundant calcite aggregates
KR8-051	312.40	Medium-grained to gritty meta-graywacke; quartz and feldspar grains show a lot of cracks; very few quartz grains with decorated PFs and only one grain with 1 set of decorated PDFs; calcite aggregates occur
KR8-052	315.75	Weakly sheared medium-grained meta-graywacke; a few quartz grains with decorated PFs (only one toasted quartz grain with 2 sets of PDFs); fractures filled with iron oxides and calcite occur
KR8-053	316.97	Sheared medium-grained meta-graywacke breccia; many decorated PFs and PDFs (1 or 2 sets) in partially or totally toasted quartz grains; abundant calcite veins and aggregates
KR8-054	320.62	Altered, fractured, mylonitic medium-grained meta-graywacke; a few decorated PFs and PDFs (1 set, only one grain with 2 sets) in partially toasted quartz grains; many penetrative fractures filled with iron oxides; similar to KR8-070
KR8-056	326.78	Medium-grained meta-graywacke (locally sheared); many quartz grains partially or totally toasted with decorated PFs and PDFs (1 or 2 sets); penetrative fractures filled with iron oxides
KR8-057	330.08	Altered, weakly sheared, medium-grained meta-graywacke, locally cataclastic; a few quartz grains with PFs and PDFs (1 set); low shock degree (~10 GPa); local cataclasis and veining filled with chlorite and epidote; many fractures filled with iron oxides; calcite aggregates
KR8-059	333.51	Mature heterogranular meta-graywacke, locally annealed, and brecciated; a lot of quartz grains with PDFs (1, 2, and 3 sets), some partially toasted; some penetrative fracturing
KR8-060	337.33	Sheared, fine-grained meta-graywacke (locally brecciated); a few quartz grains with decorated PFs and only two grains with PDFs (1 set); low shock degree (~5–6 GPa); calcite veins and aggregates occur
KR8-061	341.17	Unshocked heterogranular meta-graywacke; one penetrative fracture filled by iron oxides cut through the section; no diagnostic shock indicators
KR8-062	341.86	Sheared medium-grained meta-graywacke; a few quartz grains show decorated PFs and only one grain with PDFs (1 set); small calcite aggregates occur
KR8-063	343.57	Well-banded, fine-grained metasediment (bands of phyllite, slate, and fine-grained meta-graywacke); a lot of quartz grains with PFs and some with PDFs (1 or 2 sets); tabular opaque crystals and calcite pods occur
KR8-064	348.43	Phyllite with shocked quartz veins; very nice crenulation cleavage; many quartz grains show decorated PDFs (1 or 2 sets); cracks partially filled with iron oxides; many opaque minerals (pyrite)
KR8-065	352.31	Weakly sheared, heterogranular meta-graywacke; some PFs and PDFs (1 or 2 sets), some with decoration, in quartz grains
KR8-066	353.95	Altered, sheared, fractured, heterogranular meta-graywacke; many PDFs (1 or 2 sets); a large quartz vein cut through the section; penetrative fractures filled by iron oxides and chlorite occur
KR8-067	356.59	Weakly sheared, fractured, heterogranular meta-graywacke; many decorated PFs and PDFs (1 or 2 sets) in quartz grains, some partially toasted; many fractures filled with iron oxides
KR8-068	359.44	Altered, gritty meta-graywacke, locally cataclastic; a lot of PDFs (1 or 2 sets) in quartz grains (some partially toasted); many penetrative fractures filled by iron oxides and chlorite
KR8-069	361.18	Shocked (and somewhat brecciated) light greenish gray (chloritoid-rich), medium-grained meta-graywacke with granophyric material; some quartz grains with PDFs (1 or 2 sets) and some toasted; many graphic intergrowths of quartz and feldspar; calcite aggregates occur; very similar to KR8-106, KR8-121, and KR8-122a, but shocked
KR8-070	364.12	Mylonitic medium-grained meta-graywacke; a lot of PDFs (1 or 2 sets) in quartz grains (some partially toasted)
KR8-071	368.97	Mylonitic, medium-grained to gritty meta-graywacke, locally brecciated (annealed), and weakly shocked; few quartz grains with decorated PFs and PDFs (1 set); some fractures filled by iron oxides and chlorite
KR8-072	370.96	Sheared, fine- to medium-grained meta-graywacke; weakly shocked (<5 GPa); some quartz grains with subplanar fractures or PFs and a few with PDFs (1 set)
KR8-073	371.07	Medium-grained meta-graywacke; weakly shocked (<5 GPa); some quartz grains with subplanar fractures or PFs and a few with PDFs (1 set)
KR8-074	375.24	Medium-grained meta-graywacke; a lot of quartz grains with PFs and PDFs (1 or 2 sets); very similar to KR8-073, but shocked to a higher degree
KR8-075	377.78	Mylonite; unshocked
KR8-076	379.70	Weakly sheared medium-grained to gritty meta-graywacke (locally cataclastic); a few quartz grains with PDFs (1 set), some partially toasted; many fractures filled with secondary phyllosilicate minerals
KR8-077	380.98	Sheared fine-grained meta-graywacke; some quartz grains with decorated PFs and PDFs (1 or 2 sets), partially toasted; one mylonitic intercalation; minor fracturing; similar to KR8-072
KR8-078	382.17	Medium-grained to gritty meta-graywacke, partially annealed and locally cataclastic; no obvious shock effects
KR8-079	384.06	Weakly sheared heterogranular meta-graywacke; microfractures mostly filled with opaque minerals and phyllosilicate minerals; calcite veins; unshocked

Appendix 1. *Continued.* Detailed petrographic descriptions (rock name, minerals present, etc.) and depths of the 121 samples documented for this study. This table is based on optical microscopic observations of 174 thin sections.

Sample no.	Depth (m)	Petrographic description
KR8-080	384.54	Alternation of fine-grained metasediments (phyllite, slate, and meta-graywacke) with a wide quartzitic vein (~1 cm thick); many decorated PFs and PDFs in quartz (1 or 2 sets); plenty of calcite (veinlets and pods)
KR8-081	387.36	Weakly shocked and weakly sheared medium-grained meta-graywacke; a few quartz grains with PFs and PDFs (1 set; only 1 quartz grain seen with 2 sets); a large calcite vein and some calcite aggregates occur
KR8-082	387.78	Altered, sheared, weakly shocked, fine- to medium-grained meta-graywacke; some decorated PFs and PDFs (1 set; only one quartz grain with 2 sets) in quartz grains (some partially toasted); many cracks and fractures (some penetrative) filled by calcite, iron oxides, and chlorite; calcite aggregates occur
KR8-083	389.25	Altered, fractured, medium-grained to gritty meta-graywacke; only two quartz grains with 1 set of PFs each; several large penetrative fractures filled by iron oxides; some calcite veins and aggregates occur; no obvious shock effects
KR8-084	390.00	Slate/phyllite; no shock deformation
KR8-085	392.65	Altered, fractured, medium-grained to gritty meta-graywacke; only 4 quartz grains show decorated PFs; many fractures filled with iron oxides and chlorite
KR8-086	393.07	Altered, weakly shocked, heterogranular meta-graywacke; many quartz grains display decorated PFs (only 2 grains with decorated PDFs, 1 and 2 sets, respectively); some calcite aggregates occur
KR8-087	394.30	Altered medium-grained meta-graywacke; many PFs and some decorated PDFs (1 or 2 sets) in quartz grains (some partially toasted); a large penetrative fracture with halo of secondary calcite; abundant chlorite
KR8-088	395.25	Fine- to medium-grained meta-graywacke (weakly shocked); a few quartz grains show irregular fluid inclusion trails; a lot of calcite aggregates and veinlets; no obvious shock effects
KR8-089	397.30	Shocked medium-grained meta-graywacke partially brecciated; quartz grains display some decorated PFs and PDFs (1 set), some grains are partially toasted; calcite veinlets and aggregates occur; several fractures filled with iron oxides; few quartz grains contain rutile fibers
KR8-090	398.80	Weakly sheared, fine- to medium-grained meta-graywacke; no trace of shock deformation
KR8-091	400.35	Altered gritty meta-graywacke, fractured, and locally brecciated; some quartz grains with decorated PFs and PDFs (two quartz grains with 2 sets of decorated PDFs); many fractures (shock fracturing?) filled with chlorite and iron oxides
KR8-092	403.00	Altered medium-grained meta-graywacke; few quartz grains with decorated PFs and PDFs (1 set; only 2 grains seen with 2 sets); minor fracturing; calcite veinlets and aggregates occur
KR8-093	403.64	Altered gritty meta-graywacke locally cataclastic and fractured; only two quartz grains with PFs; numerous penetrative fractures, filled or not with iron oxides and chlorite; no obvious shock effects
KR8-094	404.18	Gritty meta-graywacke; a few quartz grains with PFs
KR8-095	405.34	Altered, fractured, and mylonitic fine-grained meta-graywacke; weakly shocked; mica-rich shear bands cut by a vein (impact breccia?); many fractures filled with iron oxides and/or secondary calcite; two quartz grains with shear fractures and PFs
KR8-096	406.31	Medium-grained meta-graywacke, locally brecciated, and fractured; some quartz grains with PFs and a few with PDFs (1 or 2 sets); several fractures (shock compression resulted?)
KR8-097	409.67	Altered sheared medium-grained to gritty meta-graywacke (locally annealed); no obvious shock effects
KR8-098	410.74	Medium-grained meta-graywacke (fractured); quartz grains (partially toasted) display decorated, curved, or subplanar fractures, sometimes PFs and PDFs (1 or 2 sets); a lot of fractures; a few quartz grains contain rutile fibers
KR8-099	412.92	Gritty meta-graywacke (fractured, locally brecciated, and weakly sheared); quartz grains display sets of subplanar fractures (some decorated), some PFs, and very few PDFs (1 set); many fractures filled with iron oxides
KR8-100	412.74	Unshocked, sheared, heterogranular meta-graywacke; calcite aggregates occur; no shock deformation
KR8-101	414.28	Altered gritty meta-graywacke; a few quartz grains with PFs; minor fractures filled by iron oxides; a few calcite aggregates occur
KR8-102	416.84	Monomict meta-graywacke breccia (sheared medium-grained meta-graywacke); quartz grains display rare decorated PFs and PDFs (1 set); some fractures and secondary calcite veinlets and aggregates occur
KR8-103	417.39	Heterogranular (from medium-grained to gritty) meta-graywacke and suevite; few quartz grains show decorated PFs (only one grain with 1 set of PDFs); calcite aggregates occur; suevite with mainly meta-graywacke clasts, besides, quartz, feldspar, melt particles, and calcite clasts
KR8-104	417.60	Altered, fine-grained meta-graywacke (locally cataclastic); a few quartz grains are partially toasted and display decorated PFs (only three grains with 1 set of PDFs); calcite aggregates occur
ADE-8a	418.05	Altered suevite veinlet (~1 cm thick) in fine metasediment (from phyllite to fine-grained meta-graywacke, locally mylonitic); a variety of lithic and mineral clasts: fine- to medium-grained meta-graywacke (altered), melt particles (brown in color), quartz, and calcite; few quartz grains displays PFs and only two quartz grains with decorated PDFs (1 set)
KR8-106	421.88	Light greenish gray (chloritoid-rich), medium-grained meta-graywacke with granophyric material; cuneiform-shaped intergrowths of quartz in feldspar; many calcite aggregates and veins occur; no distinct shock deformation; very similar to KR8-69, KR8-121, and KR8-122a

Appendix 1. *Continued.* Detailed petrographic descriptions (rock name, minerals present, etc.) and depths of the 121 samples documented for this study. This table is based on optical microscopic observations of 174 thin sections.

Sample no.	Depth (m)	Petrographic description
KR8-107	422.36	Altered suevite with a variety of lithic and mineral clasts: melt particles (brown in color, very heterogeneous in shape, from subangular to rounded), light gray (chloritoid-rich) medium-grained meta-graywacke (similar to KR8-106), meta-graywacke, quartz, slate and phyllite, and calcite; a few quartz grains display decorated PFs and PDFs (1 set); many calcite aggregates occur
KR8-108	424.78	Shocked heterogranular (form fine-grained to gritty) meta-graywacke (partially sheared) with a thick (~1.5 cm) quartz vein; several decorated PFs and PDFs (1 or 2 sets) in quartz grains (some are partially toasted); a large shocked quartz vein occur, cross-cut by calcite aggregates and veinlets (chlorite is also associated); a large pyrite flake
KR8-109	425.24	Gritty meta-graywacke; one quartz grains with shear fractures (penetrative fracturing); a few quartz grains show curved and subplanar PFs; fractures filled by iron oxides occur; pyrite infill of a cataclastic zone
KR8-110	429.31	Altered, shocked, brecciated, medium-grained meta-graywacke; several decorated PFs and PDFs (1 or 2 sets) in quartz grains (a few are partially toasted); calcite veinlets and aggregates occur; many fractures filled by calcite or chlorite
KR8-111	432.03	Quartz, shocked, fractured, and locally cataclastic (large vein); several fractures occur and show preferential orientations (subparallel fractures); many PFs and PDFs (1 or 2 sets) in quartz grains (locally toasted); some part of the section display cataclastic quartz (angular quartz fragments)
KR8-112	434.33	Suevite with a variety of lithic and mineral clasts: meta-graywacke (altered), slate and phyllite, quartz, calcite, and melt particles; clasts are small in size (2 mm maximum); only two quartz grains show PFs
KR8-113	434.59	Suevite with a variety of lithic and mineral clasts: fine- to medium-grained meta-graywacke (dominant, more or less altered, some show calcite veinlets and/or fractures filled with iron oxides), melt particles (brown in color; variety of shape), slate and phyllite, quartz, and calcite; a few quartz grains show decorated PFs or PDFs (1 set)
KR8-114	434.75	Suevite with a variety of lithic and mineral clasts: fine- to medium-grained meta-graywacke (more or less altered), melt particles (brown in color), slate and phyllite, quartz, and calcite; a few quartz grains show decorated PFs and only 2 grains seen with decorated PDFs (1 set); very similar to KR8-113, but with meta-graywacke clasts less abundant
KR8-115	437.37	Unshocked, altered, fine- to medium-grained meta-graywacke; calcite aggregates occur; no distinct shock deformation
KR8-117	439.87	Altered medium-grained to gritty meta-graywacke; some quartz grains with PFs and PDFs (1 or 2 sets); several opaque minerals (pyrite); a lot of chlorite; a sliver of impact breccia (suevite veinlet?)
CAN-31	440.32	Altered suevite with a variety of lithic and mineral clasts: fine- to medium-grained altered meta-graywacke, melt particles (brown in color, a large particle of ~1 cm), slate and phyllite, quartz, and calcite; a few quartz grains display PFs
KR8-119	441.87	Altered gritty meta-graywacke; a few quartz grains with PFs (no PDFs seen); penetrative fracturing filled by iron oxides, chlorite, or calcite; calcite aggregates occur
KR8-120	442.11	Altered mylonitic medium-grained meta-graywacke; some quartz grains show PDFs (1 or 2 sets); a lot of fractures filled by chlorite or calcite; a breccia veinlet cutting through the section
KR8-121	446.02	Light greenish gray (chloritoid-rich), medium-grained meta-graywacke, partially sheared, and with granophyric material; cuneiform-shaped intergrowths of quartz and feldspar; calcite aggregates; unshocked; very similar to KR8-069, KR8-106, and KR8-122a
KR8-122	446.69	Altered, weakly shocked, medium-grained meta-graywacke with intense cataclasis (locally brecciated); shock fracturing (shock pressure <8 GPa); a lot of calcite aggregates occur; no PDFs seen
KR8-122a	447.14	Light greenish gray (chloritoid-rich), medium-grained meta-graywacke, partially sheared, and with granophyric material; cuneiform-shaped intergrowths of quartz in feldspar (or poikiloblastic nature); abundant calcite aggregates and chloritoid; no shock recorded; very similar to KR8-069, KR8-106, and KR8-121
KR8-123	447.96	Altered medium-grained to gritty meta-graywacke (partially annealed); many fractures filled with calcite and chlorite; no PDFs (only 3 or 4 quartz grains with PFs)
KR8-124	449.12	Altered sheared heterogranular meta-graywacke (in part brecciated); many calcite aggregates occur; fractures filled with iron oxides; no distinct shock deformation
KR8-125	451.23	Weakly sheared medium-grained to gritty meta-graywacke; calcite aggregates; no diagnostic shock indicators